Organic & Biomolecular Chemistry

PAPER

View Article Online
View Journal | View Issue

Cite this: *Org. Biomol. Chem.*, 2015, **13**, 6353

Identification of a novel class of covalent modifiers of hemoglobin as potential antisickling agents†

A. M. Omar,*[a,b] M. A. Mahran,[c] M. S. Ghatge,[d] N. Chowdhury,[d] F. H. A. Bamane,[e] M. E. El-Araby,[a,f] O. Abdulmalik[g] and M. K. Safo*[d]

Received 23rd February 2015,
Accepted 16th April 2015

DOI: 10.1039/c5ob00367a

www.rsc.org/obc

Aromatic aldehydes and ethacrynic acid (ECA) exhibit antipolymerization properties that are beneficial for sickle cell disease therapy. Based on the ECA pharmacophore and its atomic interaction with hemoglobin, we designed and synthesized several compounds – designated as KAUS (imidazolylacryloyl derivatives) – that we hypothesized would bind covalently to βCys93 of hemoglobin and inhibit sickling. The compounds surprisingly showed weak allosteric and antisickling properties. X-ray studies of hemoglobin in complex with representative KAUS compounds revealed an unanticipated mode of Michael addition between the β-unsaturated carbon and the N-terminal αVal1 nitrogen at the α-cleft of hemoglobin, with no observable interaction with βCys93. Interestingly, the compounds exhibited almost no reactivity with the free amino acids, L-Val, L-His and L-Lys, but showed some reactivity with both glutathione and L-Cys. Our findings provide a molecular level explanation for the compounds biological activities and an important framework for targeted modifications that would yield novel potent antisickling agents.

Introduction

Sickle hemoglobin (Hb S), under low oxygen tension and/or when deoxygenated, polymerizes into rigid and insoluble fibres that cause the primary pathophysiology associated with sickle cell disease (SCD), leading to several secondary pathological effects, including, but not limited to, adhesion of red blood cells (RBCs) to tissue endothelium, oxidative stress, hemolysis of RBCs, decreased vascular nitric oxide bioavailability, inflammation, vaso-occlusion, impaired microvascular blood flow, and painful crises.[1–3]

Hemoglobin (Hb) functions in equilibrium between the unliganded or deoxygenated tense (T) state, which exhibits low affinity for ligands, and the liganded or oxygenated relaxed (R) state, which exhibits high affinity for ligands.[4–6] Unless noted otherwise, the R-state is used to represent the ensemble of relaxed Hb states that include the classical R-state, R2-state, R3-state, RR2-state, RR3-state, *etc.*[7,8] The crystal structure of Hb, either in the T- or R-state quaternary conformation, is made up of two αβ heterodimers (α1β1 and α2β2) arranged around a 2-fold axis of symmetry to form a central water cavity that is accessed *via* an α-cleft or a β-cleft. Allosteric effectors, both endogenous and synthetic, are known to bind to the central water cavity, the α-cleft, β-cleft, or the surface of the protein, and modulate the allosteric properties of Hb, leading to a further increase or decrease in its affinity for oxygen.[4,7–14] For example, the natural allosteric effector, 2,3-diphosphoglycerate (2,3-DPG), binds to the β-cleft of Hb, and preferentially stabilizes the T-state relative to the R-state and produces a low-affinity Hb.[9] Interestingly, sickle RBCs have a significantly reduced affinity for oxygen compared to normal RBCs, presumably as a result of an increased intracellular concentration of 2,3-DPG in the erythrocytes, which compensates for the lower hematocrit, leading to both increased and premature release of oxygen and concomitant RBC sickling.[15,16] This has led to a rational approach to treat the disease by shifting the Hb oxygen equilibrium curve (OEC) to the left (*i.e.*, stabilizing the R-state and/or destabilizing the T-state), producing a high-affinity Hb.[7,8,10,11,17–20] Unlike non-covalent binders of Hb, covalent binders have proven to be potential antisickling agents by increasing the oxygen affinity of Hb. Several aromatic aldehydes are known to have this allosteric property by

[a]*Department of Pharmaceutical Chemistry, Faculty of Pharmacy, King Abdulaziz University, Alsulaymanyah, Jeddah 21589, Saudi Arabia. E-mail: asmansour@kau.edu.sa*
[b]*Department of Pharmaceutical Chemistry, Faculty of Pharmacy, Al-Azhar University, Cairo 11884, Egypt*
[c]*Department of Pharmaceutical Chemistry, Faculty of Pharmacy, Alexandria University, Alexandria, Egypt*
[d]*Department of Medicinal Chemistry, School of Pharmacy and Institute for Structural Biology and Drug Discovery, Virginia Commonwealth University, Richmond, VA 23219, USA. E-mail: msafo@vcu.edu*
[e]*Department of Biochemistry, Faculty of Medicine, King Abdulaziz University, Alsulaymanyah, Jeddah 21589, Saudi Arabia*
[f]*Department of Pharmaceutical Organic Chemistry, Faculty of Pharmacy, Helwan University, Cairo 11790, Egypt*
[g]*Division of Hematology, The Children's Hospital of Philadelphia, PA 19104, USA*
†Electronic supplementary information (ESI) available. See DOI: 10.1039/c5ob00367a

forming a Schiff-base interaction in a symmetry-related fashion with the two N-terminal αVal1 nitrogens at the α-cleft of liganded Hb (in the R2-state conformation), and through several inter-subunit mediated hydrogen-bond and/or hydrophobic interactions cross-link the two α-subunits to stabilize the R-state Hb.[7,8,10,11,17–20] Of note is that effectors preferentially bind to the α-cleft of liganded Hb in the R2-state conformation because the α-cleft of the other relaxed states of Hb, including the classical R-state, is sterically crowded.[7,18] It is notable that, unlike liganded Hb or oxygenated Hb (oxyHb), binding to unliganded Hb or deoxygenated Hb (deoxyHb) appears to inhibit non-specific chloride binding and/or break inter-subunit hydrogen-bond interactions, leading to T-state destabilization.[7,18,21,22] 5-Hydroxymethyl-2-furfural (5-HMF, aka Aes-103) is one such left-shifting allosteric effector that binds to both R-state and T-state Hb, and has been shown to prevent Hb S polymerization and erythrocyte sickling.[10,17,18] 5-HMF is currently in phase II clinical studies for the treatment of SCD. A potential problem for the use of aromatic aldehydes for SCD therapy is their poor pharmacokinetic properties (due to metabolic instability of the aldehyde function as a result of aldehyde dehydrogenase metabolism) which may necessitate large amounts and frequent dosing to reach therapeutic level.[10] This has prompted several studies to find alternate covalent modifiers of Hb, such as isothiocynates and thiols, to treat the disease.[23,24]

Effectors that right-shift the OEC to produce low oxygen-affinity Hb have also been studied for treating ischemia-related cardiovascular diseases, where more oxygen is needed to heal tissue or organs, and also as radiation enhancers in the radiotherapy of hypoxic tumors.[25–28] Right-shifters encompass both covalent binders, such as aromatic aldehydes,[29,30] and non-covalent binders, *e.g.* aromatic propionates.[12,13,31–34] Structural studies of these effectors show that the compounds stabilize the T-state through inter-subunit or cross-linking interactions.[12,13,31–34] Some of these right-shifters have also been shown to bind to R-state Hb and destabilize this conformation.[34–36] From the foregoing, it is clear that Hb effectors can bind both T-state and R-state Hb; however, the direction of the OEC shift is dependent on which Hb state is preferentially stabilized and/or destabilized.

Ethacrynic acid (ECA), used as a diuretic, also increases the oxygen affinity of Hb and/or causes stereospecific inhibition of polymer formation with a concomitant antisickling effect.[37,38] In contrast to aromatic aldehydes, the antisickling activity of ECA is through interaction with the surface-located Hb residue, βCys93 *via* a Michael addition reaction. Unfortunately, the diuretic activity of ECA precludes its use as an oral therapeutic agent for the treatment of SCD. The current study was initiated with the principle of forming a similar covalent adduct between imidazolylacryloyl derivatives (designated as KAUS molecules) and βCys93 that not only would increase the oxygen affinity of Hb, but do so with greater antisickling potency than ECA, as well as with reduced or no diuretic effect. We also posited that these compounds, with a reactive α,β-unsaturated ketone, would be more metabolically stable than aromatic aldehydes, necessitating lower and less frequent doses. Biological analysis, including OEC and sickle RBC morphological antisickling studies, showed the compounds to exhibit weak or no allosteric and antisickling activities when compared to ECA. Structural study of Hb in complex with two of the compounds, KAUS-12 and KAUS-15, provides molecular insight into the unexpected biological effect, and offers important direction and guidance for structure-based redesign of the compounds to yield potent left-shifting and antisickling agents.

Results

Design

Ethacrynic acid increases Hb affinity for oxygen, and expectedly shows antisickling properties.[37,38] In a reported crystallographic study of ECA complexed to deoxyHb, it was shown that the β-unsaturated carbon of the effector reacted covalently with the sulfur atom of βCys93 (Michael addition reaction; Scheme 1), while the rest of the molecule makes hydrogen-bond and/or hydrophobic interactions with αPro44, βAsp94, βHis97, and αThr41.[38] The interaction at the βCys93 binding site destabilizes the T-state by abolishing a salt-bridge interaction between βHis146 and βAsp94 in deoxyHb, shifting the allosteric equilibrium to the R-state and increasing the protein affinity for oxygen. Binding of ECA to the surface-located βCys93 was also suggested to prevent stereospecific interaction between Hb S molecules, providing a secondary antisickling effect.[38] Alkyl isothiocynates,[23] and quite recently thiols,[10,24] have also been shown to covalently bind to βCys93, acting in a similar mechanistic manner as ECA to increase Hb affinity for oxygen. Using ECA as a scaffold, we rationally designed and synthesized nine imidazolylacryloyl derivatives with varying chloro-substitutions on the phenyl ring, as well as varying carboxylate arm lengths (Fig. 1). These compounds have similar a Michael acceptor chemotype α,β-unsaturated ketone as ECA, and it was expected that the β-unsaturated carbon would react in a similar covalent manner to ECA, *i.e.*, undergoing a Michael addition reaction with the sulfur of βCys93. The replacement of the ethyl group attached to the β-unsaturated carbon in ECA with an imidazole in the KAUS molecules

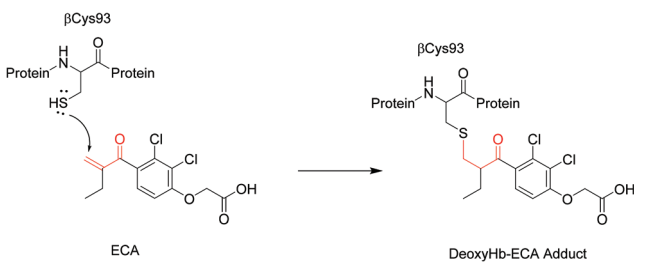

Scheme 1 Schematic representation of the Michael addition reaction between the β-unsaturated carbon of ethacrynic acid (ECA) and the βCys93 sulfur of deoxyHb.

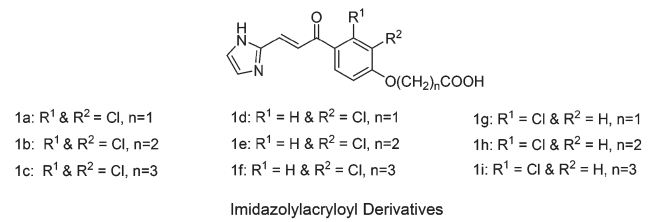

Fig. 1 Synthesized imidazoloylacryloyl derivatives.

was also anticipated to increase the reactivity of the β-carbon and hence accelerate the Michael addition reaction. It was also envisaged that the hydrophobic chlorobenzene ring, imidazole ring and/or the varying carboxylate moiety would make various hydrogen-bond/hydrophobic interactions with the βCys93 binding pocket residues, including αLys40, αThr41, αSer49, αPro44, βGlu90, βAsp94, βHis97, and the C-terminal residue βHis146, which would confer binding stability to these compounds, and hence a greater destabilization effect on the T-state, leading to greater increase in Hb oxygen affinity when compared to ECA.

Chemistry

For the phenoxyacetic acid and phenoxybutyric acid derivatives (**1a**, **1c**, **1d**, **1f**, **1g** and **1i**), the synthetic sequence in Scheme 2 was followed, where the alkylation step was carried out using the corresponding bromo-ethyl esters.[39,40] The ester intermediate **3** was hydrolyzed to obtain the corresponding acid intermediate **4** that was used for the condensation step. The condensation of methylketone intermediate **4** with trityl-protected imidazole-3-carbaldehyde **5**[41] was accomplished under catalysis by sodium hydroxide to give the protected imidazolylacryloyl final precursors **6**.[42,43] The target phenoxyacetic and phenoxybutyric acid derivatives were obtained after removal of the trityl protecting group under standard acidic conditions.[44]

A modified synthetic route (Scheme 3) was used for the propionic acid derivatives **1b**, **1e** and **1h**, since the alkylation of the hydroxyl group using ethyl-3-bromopropionate was not successful. The protected aldehyde, 2-(2-bromoethyl)-1,3-dioxolane was used for alkylation as a precursor for the acid. The acid intermediate **8** was obtained by deprotecting the cyclic acetal using aq. HCl, followed by oxidation using oxone.[45] The final products (**1a–1h** and **1i**) were purified using silica gel column chromatography to give purities >95% as indicated by HPLC (UV detection) and/or LC-MS.

Oxygen equilibrium curve (OEC) studies

Compounds that increase the oxygen affinity of Hb are expected to shift the OEC to the left, and the degree of shift is reported as an increase or decrease in P_{50} (the oxygen tension at 50% Hb O_2 saturation), while the degree of allosteric character is indicated by the slope of the oxygen binding curve (n_{50}). The effect of the nine KAUS molecules on Hb affinity for oxygen was determined using normal human blood and multipoint tonometry as previously reported,[18] and the results are shown in Table 1. At 2 mM concentration, the compounds showed very little or no left-shifting effect on the OEC (0.0–2.8 mmHg) compared to the 5.7 mmHg left-shift by ECA. One compound, KAUS-10, seems to right-shift the OEC by 2.1 mmHg. There appears to be some correlation in the OEC shift and the varying carboxylate arm length in the three classes of compounds, where the phenoxybutyrates (with a longer carboxylate arm) seem to give the greatest shift to the left, while the phenoxyacetates (with a shorter carboxylate arm) show the smallest shift, and in some instances even right-shifts the OEC. There is no apparent correlation between the allosteric activity of the compounds and the varying chloro-substitutions on the phenyl ring.

Antisickling studies

Compounds that increase the oxygen affinity of Hb are expected to inhibit RBC sickling.[7,8,11,18] Selected compounds, including KAUS-12, KAUS-13, KAUS-15, KAUS-16, and

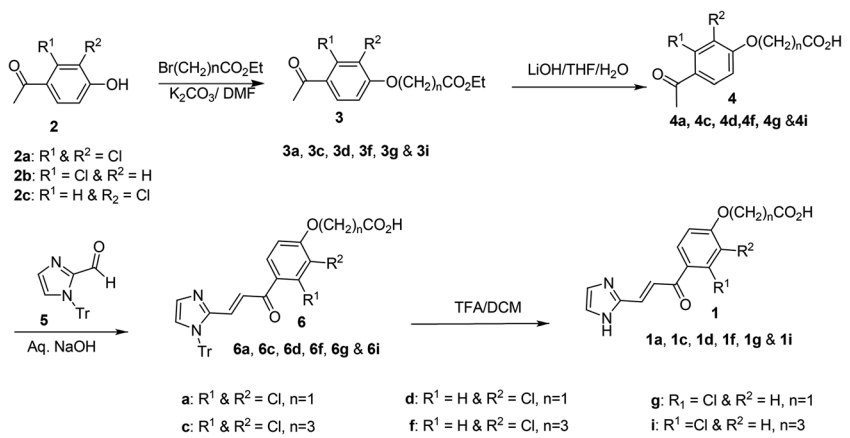

Scheme 2 Synthetic scheme for compounds **1a**, **1c**, **1d**, **1f**, **1g** and **1i**.

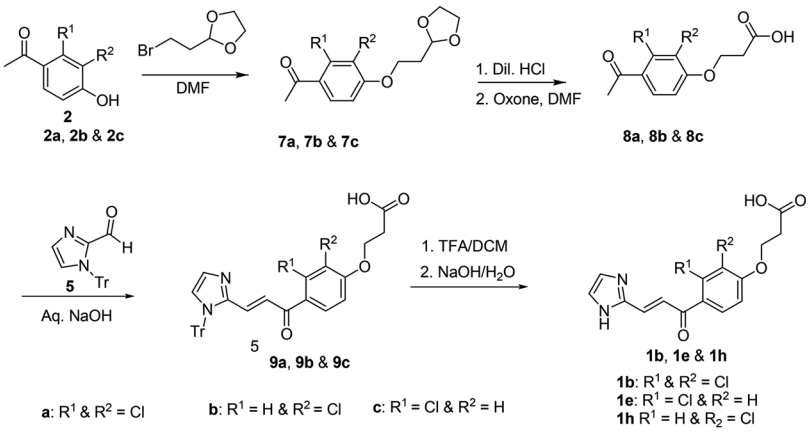

Scheme 3 Synthetic scheme for compounds **1b**, **1e** and **1h**.

Table 1 The effect of compounds on Hb affinity for oxygen using normal whole blood[a]

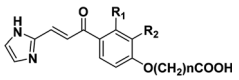

Comp	Name	R_1	R_2	N	Mean P_{50}[b]	Ave. dev. from mean	ΔP_{50}[c]	n_{50}[d]
Ctr	DMSO[e]				38.3	0.0	0.0	2.3
Ctr	ECA				32.7	0.2	−5.7	1.9
1a	KAUS-10	Cl	Cl	1	40.4	0.23	2.1	2.2
1b	KAUS-11	Cl	Cl	2	38.1	0.47	−0.2	2.2
1c	KAUS-12	Cl	Cl	3	36.9	0.14	−1.4	1.9
1d	KAUS-13	H	Cl	1	37.4	0.05	−1.0	2.4
1e	KAUS-14	H	Cl	2	38.2	0.3	−0.1	2.1
1f	KAUS-15	H	Cl	3	35.6	0.55	−2.8	1.9
1g	KAUS-16	Cl	H	1	38.3	0.74	0.0	2.3
1h	KAUS-17	Cl	H	2	37.8	0.15	−0.5	2.3
1i	KAUS-18	Cl	H	3	37.4	0.42	−0.9	2.1

[a] The results are the means of 2 measurements. [b] P_{50} is the oxygen pressure at which normal RBCs (22% hematocrit) are 50% saturated with oxygen. [c] ΔP_{50} is P_{50} of compound-treated cells – P_{50} of control. [d] n_{50} is the Hill coefficient at 50% saturation with oxygen. [e] The final concentration of DMSO was about 2% in all samples, including the control.

KAUS-17, at 2 mM concentration were tested for their abilities to prevent RBC sickling under hypoxic conditions.[11,18] As expected from the weak or no left-shifting activities, the compounds showed very little to no observable antisickling effect, with even KAUS-16 and KAUS-17 promoting slight RBC sickling (Fig. 2). In comparison, the control ECA inhibited about 18% RBC sickling.

Co-crystallization of deoxygenated Hb or carbonmonoxy Hb with KAUS-12 or KAUS-15

X-ray crystallography was used to determine the binding site of KAUS-12 and KAUS-15 in both deoxygenated Hb and carbonmonoxy Hb (COHb) to explain the unexpected biological activities of the imidazolylacryloyl derivatives. The compounds were first reacted with deoxyHb or carbonmonoxy Hb (COHb), followed by crystallization using high-salt conditions as previously described.[11,18,22,46] Unlike aromatic aldehydes, which co-crystallize with deoxyHb to give both T- and R2-state crystals,[11,18] we only observed T-state crystals during the co-crystallization experiment with deoxyHb. The T-state crystals are isomorphous with the native deoxyHb crystal (PDB code 2DN2), necessitating the use of 2DN2 as the starting model for the refinement of both complex structures. The two structures refined to 1.7 Å and 1.9 Å, respectively, and the structural statistics are summarized in Table 2. The refined KAUS-12 and KAUS-15 complex structures are deposited in the PDB with the ID codes 4ROL and 4ROM, respectively.

The co-crystallization experiment of KAUS-15 or KAUS-12 with COHb resulted in the formation of classical R-state crystals that diffracted to 2.0 and 2.8 Å, respectively. The isomorphous R-state native COHb structure (1LJW) was used as the starting model to refine the complexes. Unlike the deoxyHb complex structures, which showed apparent binding of the KAUS compounds (see below), none of the COHb structures showed bound compound. Since the liganded structures did not have any bound effector, and were also determined to be indistinguishable from the native 1LJW structure, the refinements were terminated at R_{factor}/R_{free} of 23.5/26.4 and 26.4/33.5, respectively.

KAUS compounds bind at the α-cleft of deoxygenated Hb with the amine of the N-terminal αVal1

We assumed, based on the ECA interaction with Hb, that the primary site of reaction of the KAUS molecules would be at the βCys93 binding site; however, the crystallographic studies with KAUS-12 and KAUS-15 showed no apparent binding of either compound to βCys93 in the classical R-state or T-state structures. Instead, we observed that the compounds were bound at the α-cleft of the T-state structures (Fig. 3A and B). There was no apparent binding of the compounds at the α-cleft of the classical R-state structures, which we attribute to steric crowding at this binding pocket.[7,18]

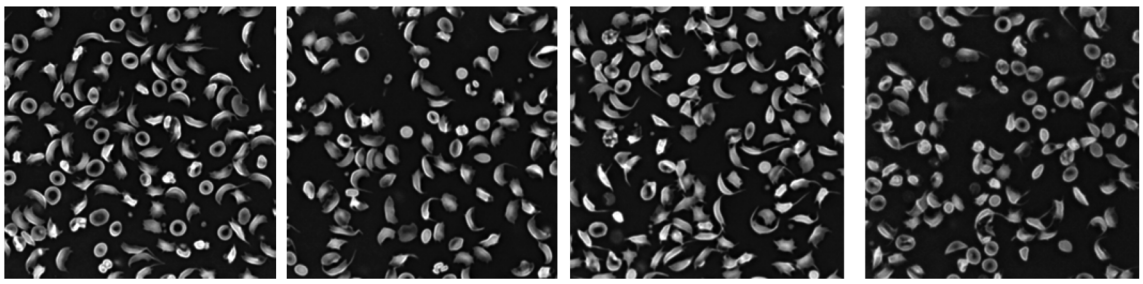

Fig. 2 Morphology of SS cells after incubation with various compounds (2 mM) or without compound under 4% oxygen at 37 °C for 5 h. (A) In the absence of a test compound, most of the cells underwent sickling (85%). (B) At 2 mM, most of the compounds, including KAUS-15 depicted here, showed very little or no observable antisickling effect. (C) At 2 mM, KAUS-16 promoted sickling of the cells. (D) At 2 mM, ECA inhibited sickling of the cells by ~18%.

Table 2 Crystallographic data and refinement statistics for deoxyHb in complex with KAUS-12 and KAUS-15; values in parentheses refer to the outermost resolution bin

Data collection statistics	KAUS-12	KAUS-15
Space group	$P2_1$	$P2_1$
Cell dimensions (Å)	a = 61.64, b = 76.57, c = 53.20; β = 98.02	a = 61.98, b = 78.92, c = 53.26; β = 98.44
Resolution (Å)	33.59–1.70 (1.76–1.70)	33.75–1.90 (1.97–1.90)
No. of measured reflections	159 264	134 725
Unique reflections	52 644 (5225)	37 044 (3482)
Redundancy	3.03 (3.03)	3.64 (3.80)
$I/\sigma I$	8.4 (4.4)	22.7 (5.0)
Completeness (%)	97.7 (96.8)	92.5 (87.8)
R_{merge} [a] (%)	7.4 (19.3)	3.4 (16.3)
Structure refinement		
Resolution limit (Å)	33.59–1.70 (1.78–1.70)	33.18–1.90 (1.99–1.90)
No. of reflections	52 489 (6138)	37 014 (4143)
R_{work} (%)	18.2 (27.0)	21.3 (30.6)
R_{free} [b] (%)	20.6 (30.1)	24.8 (34.2)
R.m.s.d. standard geometry		
Bond lengths (Å)	0.008	0.008
Bond angles (°)	1.5	1.4
Dihedral angles (%)		
Most favored regions	93.2	93.0
Allowed regions	6.8	7.0
Average B-factors (Å^2)		
All atoms	16.0	29.7
Protein alone	13.5	28.1
Water	29.7	39.6
KAUS	34.9	51.4
Heme	10.3	23.8

[a] $R_{mege} = \sum_{hkl}\sum_i/I_{hkli} - \langle I_{hkli}\rangle/\sum_{hkl}\sum_i \langle I_{hkli}\rangle$. [b] R_{free} was calculated with 5% excluded reflection from the refinement.

The deoxyHb complex structures of KAUS-12 and KAUS-15, and the native deoxyHb 2DN2 structure, are quite similar to each other, with a root mean square deviation (rmsd) of ~0.4 Å, indicating no significant change in the overall T-state quaternary conformation upon effector binding. Similarly, there are no apparent differences in the heme environments, the interdimer interfaces, or the inter-subunit hydrogen-bond/salt bridge interactions that are unique to T-state Hb. Thus, the overall quaternary and tertiary structures are very similar among the three T-state structures.

Although the compounds bind to T-state Hb, they are characterized by weak and highly disordered electron densities (Fig. 3C–F). There are several reported cases where bound left-shifting effectors at the α-cleft of deoxyHb show weak and disordered density even though these compounds bind covalently to the protein.[11,18] This is in contrast to right-shifting effectors, especially very potent ones, which are normally well-ordered as a result of extensive inter-subunit mediated interactions with the protein.[12] Since the bound compound densities are weak, their refined positions may not be totally

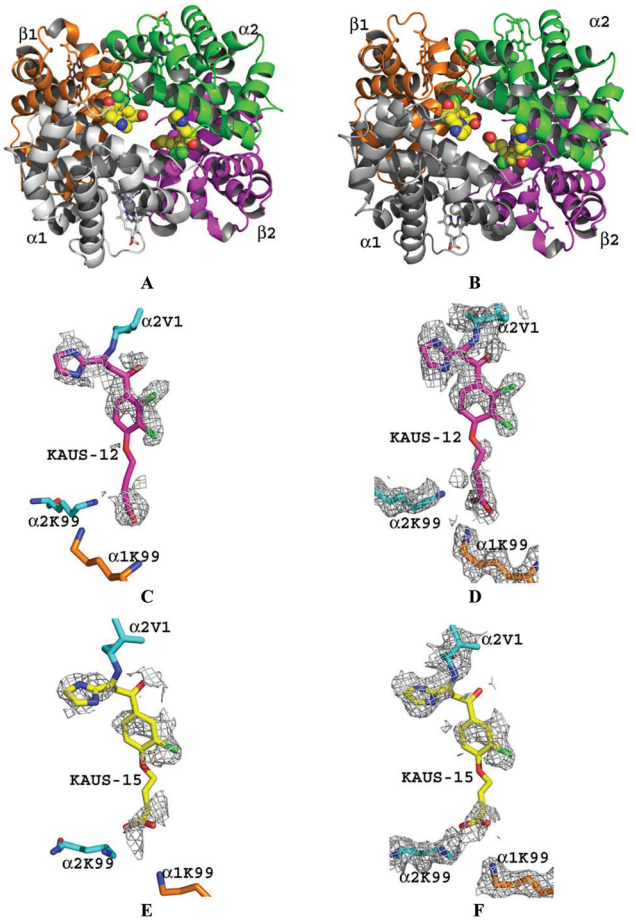

Fig. 3 Binding of KAUS-12 and KAUS-15 at the α-cleft of deoxyHb. (A) Symmetry-related bound KAUS-12 (spheres) at the α-cleft of deoxyHb (ribbons). (B) Symmetry-related bound KAUS-15 at the α-cleft of deoxyHb. (C) Difference electron density ($F_o - F_c$) map of the bound KAUS-12 (before KAUS-12 was built into the model) contoured at 2.2σ. (D) Final $2F_o - F_c$ map of the bound KAUS-12 contoured at 0.7σ. (E) Difference electron density ($F_o - F_c$) map of the bound KAUS-15 (before KAUS-15 was built into the model) contoured at 2.2σ. (F) Final $2F_o - F_c$ map of the bound KAUS-15 contoured at 0.7σ.

unambiguous, and therefore only general conclusions for compound–protein interactions will be made.

For each T-state complex, we identified two-symmetry-related difference electron densities close to α1Val1 and α2Val1 (Fig. 3C–F). At each binding site, the αVal1 nitrogen makes a covalent interaction with the β-unsaturated carbon through a Michael addition reaction (Fig. 4A), which is ascertained by an overlapping electron density of the two interacting atoms (Fig. 3C–F). With a covalent interaction with one of the αVal1 nitrogens (such as α2Val1), the imidazole ring of KAUS-12 or KAUS-15 is in a position to make either direct or water-mediated intra-subunit hydrogen-bond interaction with the α2Ser131 and α2Thr134 hydroxyl groups (Fig. 4B and C). The α,β-unsaturated ketone and the chlorophenyl ring moieties could also make both intra-subunit and inter-subunit hydrophobic interactions with the surrounding residues, α2Lys127, α2Ala130, α1Thr137, α1Ser138, α1Tyr140, α1Arg141 and β2Trp37. The butyrate, which is directed toward the middle of the central water cavity, could also make direct and/or water-mediated inter-subunit and intra-subunit hydrogen-bond/salt-bridge interactions with the surrounding residues, α1Lys99, α2Lys99, α1Pro95, α1Arg141, and α1Asp126. Similar interactions as discussed above for the α2Val1 bound molecule are also observed for the symmetry-related α1Val1 bound molecule.

From the foregoing, it is apparent that the symmetry-related molecules of KAUS-12 or KAUS-15 bind to the α-cleft of deoxyHb, making possible hydrogen-bond/hydrophobic mediated interactions that tie the two α-subunits together to stabilize the T-state Hb. These cross-link interactions are reminiscent of monoaldehyde-monocarboxylate, monoaldehyde-biscarboxylate, and bisaldehyde-biscarboxylate molecules that also bind to deoxyHb and confer a similar stabilization effect on T-state Hb.[29,30] The above observations are in contrast with yet another class of aromatic aldehydes (monoaldehydes), *e.g.* 5-HMF, that bind to both deoxyHb and liganded Hb (in the R2-state form), but while these compounds confer stability to the R-state Hb through mediated inter-subunit interactions, binding to deoxyHb destabilizes the T-state, and as a result the allosteric equilibrium is shifted to the R-state Hb.[7,11,18]

Reactivity of KAUS toward glutathione (GSH) and free amino acids, L-Cys, L-Val, L-His and L-Lys

Although the structural studies suggest specific binding of the compounds at the α-cleft of Hb, nevertheless, due to their highly reactive Michael acceptor moiety, there is a likelihood of non-specific binding to a number of nucleophiles, including GSH and other amino acids on proteins. We therefore investigated possible GSH, L-Cys, L-Val, L-His or L-Lys conjugates with KAUS-12, KAUS-15 or ECA using LC-MS or UPLC-MS analysis.

The LC-MS analysis of the reaction between KAUS-12 and GSH after 1 h showed only traces (1.6%) of the adduct ion, which increased to 9.7% after 3 h (Fig. S1A,† Table 3). A similar result was observed with KAUS-15, which showed 10.6% and 18.6% of the adduct ion at 1 h and 3 h, respectively (Fig. S1B,† Table 3). In contrast to the KAUS compounds, ECA reacted strongly with GSH, disappearing completely after 60 minutes of reaction, and only its GSH adduct was observed in the mass (Fig. S1C†).

The UPLC-MS analysis of the reactions between the compounds (KAUS-12, KAUS-15 and ECA) and the four amino acids, L-Cys, L-Val, L-His and L-Lys (which were incubated for 3 hours) showed only L-Cys reacting in any significant manner with the three compounds (Table 4; Fig. S2–S5†). ECA was the most reactive toward L-Cys (~96%), followed by KAUS-15 (~57%), while KAUS-12 showed the least reactivity (~32%). Interestingly, the KAUS compounds were unreactive toward L-Val, L-His and L-Lys (Table 4; Fig. S2–S5†) even though structural studies suggest adduct formation with the N-terminal valine of the protein. Similar observations have been reported with aromatic aldehydes, where the Schiff base equilibrium constants between the aldehyde and the amine of the N-term-

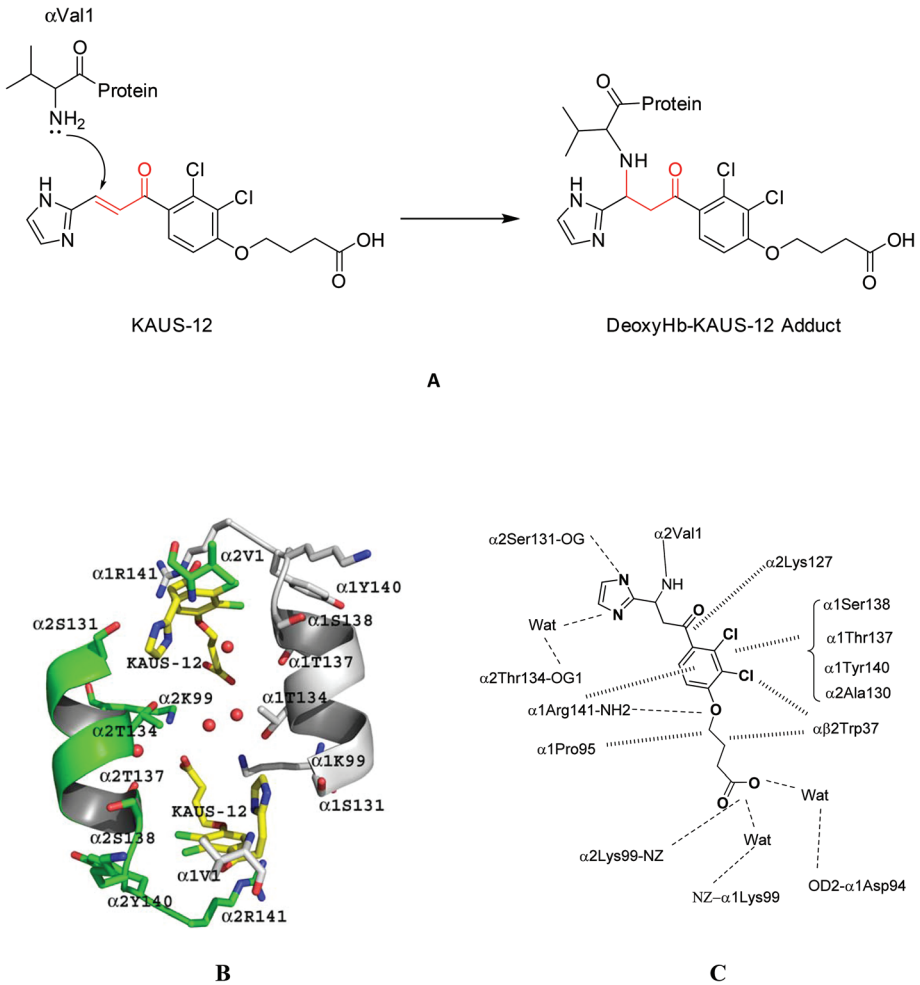

Fig. 4 Interactions between the protein and KAUS-12 or KAUS-15. (A) Schematic representation of the Michael addition reaction between the αVal1 nitrogen of Hb and the β-unsaturated carbon of the KAUS molecule. (B) Possible interactions between the protein and the KAUS-12 molecule at the α2Val1 binding site. For clarity, not all surrounding residues are shown. (C) Schematic representation of the possible interactions between KAUS-12 and deoxyHb at the α2Val1 binding site. Note that atomic distances are not given because of the uncertainty in the atomic positions of the bound compound as a result of the weak density.

Table 3 LC-MS measurements of relative ratios of KAUS-12, KAUS-15, and ECA and their adduct products with GSH

Reaction time (min)	Peak	RT[a] (min)	Max. *m/z*	Area	Ratio of Cpd/adduct (%)
KAUS-12					
60	Compound	3.2	368.9	223 754 007	98.4
	Adduct	2.4	454.3	3 682 173	1.6
180	Compound	3.1	368.9	136 800 833	90.3
	Adduct	2.4	454.2	14 624 755	9.7
KAUS-15					
60	Compound	2.9	334.9	151 292 991	89.4
	Adduct	2.4	642.2	17 918 962	10.6
180	Compound	2.9	334.9	156 535 264	81.4
	Adduct	2.3	642.2	35 710 465	18.6

[a] RT = Retention time.

inal Val1 of Hb are 3- to 5-fold greater than typical Schiff base equilibrium constants with free amino acids or small molecule amines.[20] We note that ECA has been reported to form a covalent interaction with another surface located Hb residue, βHis117;[38] however, it only showed very weak reactivity with free L-His (3%). Similar to the KAUS compounds, ECA was unreactive toward L-Val and L-Lys. The apparent reactivity of the KAUS compounds, as well as aromatic aldehydes and ECA, with the protein amino acids but not with the corresponding free amino acids could be due to the fact that the protein offers stable binding environments for these compounds that contribute to the stability of the covalent interactions.

Reactivity of KAUS-15 towards βCys93 of Hb

Both solution and structural studies suggest ECA forms a covalent interaction with βCys93 of Hb,[37,38] consistent with the strong reactivity of this compound with free L-Cys. Our structural studies on the other hand show no adduct formation with βCys93, even though the compounds do react with free cysteine, although more weakly than ECA. We therefore conducted a solution-based sulfhydryl assay with Hb incubated

Table 4 UPLC-MS measurements of relative ratios of KAUS-12, KAUS-15, and ECA and their adduct products with different amino acids

Amino Acid	Compound	Peak	RT[a] (min)	Max. *m/z*	Area	Ratio of Cpd/adduct
Cysteine	Ethacrynic acid	Compound	4.43	302.7	898	3.7
		Adduct	2.63	423.7	23 733	96.3
	KAUS-12	Compound	2.45	368.7	19 901	67.5
		Adduct	1.79	489.7	9559	32.5
	KAUS-15	Compound	2.12	334.8	14 150	42.8
		Adduct	1.34	455.8	18 915	57.2
Lysine	Ethacrynic acid	Compound	4.42	302.7	11 524	100
		Adduct	N/A	N/A	N/A	N/A
	KAUS-12	Compound	2.46	368.8	21 520	100
		Adduct	N/A	N/A	N/A	N/A
	KAUS-15	Compound	2.13	334.9	22 750	100
		Adduct	N/A	N/A	N/A	N/A
Valine	Ethacrynic acid	Compound	4.42	302.8	13 128	100
		Adduct	N/A	N/A	N/A	N/A
	KAUS-12	Compound	2.46	368.8	31 545	100
		Adduct	N/A	N/A	N/A	N/A
	KAUS-15	Compound	2.15	334.9	23 461	100
		Adduct	N/A	N/A	N/A	N/A
Histidine	Ethacrynic acid	Compound	4.42	302.8	12 934	97.1
		Adduct	1.71	457.9	382	2.9
	KAUS-12	Compound	2.46	368.8	29 432	100
		Adduct	N/A	N/A	N/A	N/A
	KAUS-15	Compound	2.16	334.8	17 020	100
		Adduct	N/A	N/A	N/A	N/A

[a] RT = Retention time.

with KAUS-15 (which showed greater reactivity with free cysteine than KAUS-12) and 5,5′-dithiobis-(2-nitrobenzoic acid) (DTNB) to determine the KAUS reactivity with βCys93. First, we measured the accessible thiol content in Hb, which was found to be close to two, consistent with previous reports that suggest that out of the six thiols present in Hb, only the two βCys93 are solvent accessible and reactive.[47] As expected, in the presence of ECA, almost 100% of the βCys93 thiols were no longer detectable, indicating complete reaction of ECA with the βCys93 thiols. In the presence of KAUS-15, about 78% of the thiol groups were available to react with DTNB, suggesting a weak interaction between KAUS-15 and βCys93, perhaps explaining why the KAUS compounds were not observed crystallographically at the βCys93 binding site. It should be noted that several compounds, including thiols and alkyl isothiocynates, have been shown crystallographically to form a covalent interaction with βCys93 of Hb.[10,23,24]

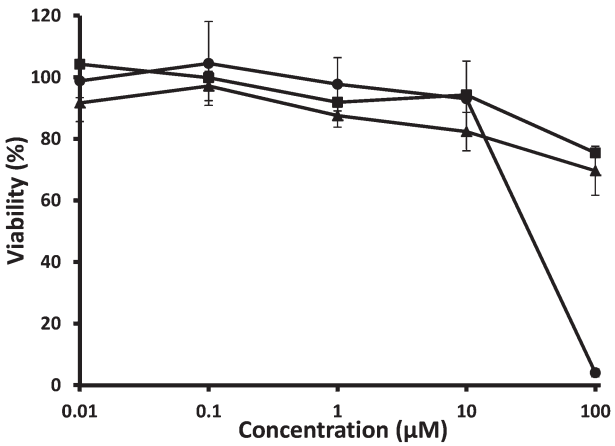

Fig. 5 Toxicity of compounds in the C-166 mouse fibroblast cell line, assessed using the SRB assay. Results are shown for KAUS-12 (squares) and KAUS-15 (triangles), in comparison to ECA (circles). The error on each data point is the standard deviation of three measurements.

Cytotoxicity of KAUS

We determined the potential toxicity of KAUS-12, KAUS-15, and ECA by testing against the C-166 mouse fibroblast cell line using the cell viability sulforhodamine B (SRB) assay,[46] following compound incubation in a concentration range from 0.01 μM to 100 μM over a 72 h period. While ECA contributes to cell toxicity with an IC_{50} of 22 μM, the two tested compounds were much less toxic (Fig. 5). When extrapolated from the data, the IC_{50} values of both KAUS-12 and KAUS-15 were greater than 1.6 mM.

Discussion

One therapeutic strategy for SCD is to develop allosteric effectors of Hb that stabilize the relaxed state Hb and/or desta-

bilize the tense state Hb to increase the concentration of the high-oxygen-affinity Hb species that do not polymerize.[7,10] Finding such Hb allosteric molecules has been a challenge, due in part to the difficulty of designing pharmaceutically useful agents capable of modifying the large amounts of intracellular Hb (~5 mmol L^{-1}). However, this fact is alleviated by the knowledge that therapeutic efficacy could be obtained with 50% or less modification of Hb S, as evidenced by patients who are heterozygous for SCD and are asymptomatic, as well as by the fact that patients that produce about 20% fetal Hb (Hb F) only have the mild form of the disease.[48–50] Nonetheless, it would still require significant amounts of compounds to treat the disease, underscoring the realization that any potential antisickling agent would have to be highly specific for Hb, as well as exhibit a long and sustained effect. One class of allosteric effectors, aromatic aldehydes, have become attractive since they form a covalent, albeit transient, interaction with the α-subunit N-terminal αVal1 nitrogens of Hb, which leads to significant reduction of Hb S polymerization due to the ability of the compounds to increase Hb S oxygen affinity.[10,11,17–19] Unfortunately, the metabolic instability of aromatic aldehydes, as a result of aldehyde dehydrogenase oxidation of the aldehyde functional group to the corresponding inactive acid analog, makes the use of these compounds to treat a large amount of Hb problematic. We now report a new class of Hb covalent binding effectors, imidazolylacryloyl derivatives, that were designed based on the ethacrynic acid pharmacophore to form a covalent adduct with the surface-located amino acid βCys93. We posited that this interaction should increase the protein oxygen affinity and/or stereospecifically prevent polymer contacts. It was also anticipated that the metabolically stable functional group and the covalent interaction with Hb would lead to both lower compound doses and a longer sustained therapeutic action.

Nine compounds, named KAUS, were successfully synthesized (Fig. 1; Table 1; Schemes 2 and 3) and tested for their effect on Hb oxygen binding properties, as well as their antisickling properties. Unexpectedly, the compounds showed no or only weak biological effects compared to ECA (Fig. 2; Table 1). Some of the compounds even showed the opposite pharmacological effect by decreasing Hb affinity for oxygen and/or promoting cell sickling. To understand the unexpected behavior of these compounds on an atomic level, two of the compounds KAUS-12 and KAUS-15 were co-crystallized with liganded Hb (COHb) and unliganded Hb (deoxyHb) and the structures determined.

Contrary to our design expectation that the KAUS molecules would form a covalent adduct with βCys93 (Scheme 1), the structural studies with both deoxyHb and COHb showed no observable binding at βCys93. Rather, the studies with deoxyHb showed KAUS-12 and KAUS-15 to bind covalently in a symmetry-related fashion at the α-cleft of the Hb *via* a Michael addition reaction that involved the β-unsaturated carbon and the αVal1 nitrogens of Hb (Fig. 3 and 4). Notably, the two compounds make both intra-subunit and inter-subunit interactions; the latter interactions, which cross-link the two α-subunits, are expected to further stabilize the T-state Hb and decrease the protein affinity for oxygen.

While βCys93 is buried in deoxygenated Hb, it is accessible in liganded Hb and able to react with electrophiles.[10,24] A thiol containing compound was recently shown crystallographically to form a covalent adduct with βCys93 in classical R-state Hb and R3-state Hb.[24] However, as noted above, we did not observe any KAUS compound at the βCys93 binding site in the classical R-state structure, even though our solution studies suggest possible binding of the compounds with this amino acid, albeit weak. This weak binding may explain why the compounds were undetected in our liganded crystal structure. Unlike the T-state structure, which showed the KAUS compound bound to the N-terminal αVal1 nitrogen, we did not observe such binding in the classical R-state structure, consistent with the sterically hindered α-cleft of R-state Hb precluding binding at this pocket.[7,18] Instead, effectors that bind to the α-cleft of liganded Hb are known to bind to the R2-state form[7,11,18] Although we have not been able to obtain liganded Hb crystals in the R2-state, we speculate that the KAUS compounds like aromatic aldehydes also bind to the α-cleft of R2-state Hb.

The fact that in general we do not observe a right-shifting effect suggests that the interaction of the compounds with liganded Hb leads to stabilization of the R-state, as observed for several potent left-shifting antisickling aromatic aldehydes that are known to bind to both R-state Hb and T-state Hb.[7,11,18] Nonetheless, these aromatic aldehydes, unlike the KAUS molecules, do not add to the T-state stabilization, explaining their potent left-shifting properties.[7,11,18] We also note that while aromatic aldehydes bind to liganded Hb with strong and well-resolved electron density, like the KAUS compounds, their location in deoxyHb is characterized by very weak and broken densities.[7,11,18]

The nine imidazolylacryloyl derivatives differ by having varying chloro-substitutions on the phenyl ring and/or varying carboxylate arm lengths. Although subtle, the compounds with the longest and most flexible carboxylate arm length, *i.e.* the phenoxybutyrates (*e.g.* KAUS-12 and KAUS-15), appear to shift the OEC the most to the left, while the shortest and least flexible, *i.e.* the phenoxyacetates (*e.g.* KAUS-10), shift the OEC the least to the left or even shift it to the right. αLys99, which is quite flexible, can easily move to interact with the varying chain-length carboxylates, and these interactions as noted above are expected to stabilize the T-state. Most likely, the flexible phenoxybutyrates will make weaker inter-subunit interactions with αLys99, and thus confer less constraint on the T-state, while the shorter chain phenoxyacetates will make a tighter interaction with αLys99 and confer more stability to the T-state, consistent with the trend in the allosteric properties. From the foregoing, the carboxylates may be responsible for most of the inter-subunit interactions that stabilize the T-state, and removing them would presumably generate novel covalent effectors that would still bind at the α-cleft. However, instead

of stabilizing the T-state they would rather destabilize it, shifting the allosteric equilibrium to the R-state and exhibit a potent antisickling effect. Indeed, left-shifters, which covalently bind at the α-cleft, do not have carboxylates, while the opposite is true for right-shifters.[7,8,10,18,29,30]

The question we pose is why do the KAUS compounds form a covalent adduct with the N-terminal αVal1 amine, while ECA (also with a β-unsaturated carbon) preferentially forms a covalent adduct with the βCys93 thiol? First, the weakly nucleophilic αVal1 amino group, which may have been unreactive to the alkylacryloyl β-unsaturated carbon of ECA, has now become susceptible to electrophilic attack by the highly reactive imidazolylacryloyl (arylacryloyl) β-unsaturated carbon. Consistent with when an electrophile (*e.g.* isothiocyanate or aldehyde) is directly attached to an aromatic ring (as observed in aromatic aldehydes or aryl isothiocyanates), these compounds are known to preferentially bind to the N-terminal amines of the α-chain of Hb.[11,18,23,29,30] On the other hand, if the electrophile is attached to an alkyl group, as observed in ethacrynic acid, alkyl isothiocyanates or alkyl aldehydes, the compound does not bind to the α-cleft, with ethacrynic acid and alkyl isothiocyanates known rather to react with βCys93.[23,37,38] Second, and very importantly, the α-cleft seems to offer a highly specialized complementary binding pocket for different classes of Hb effectors that include aromatic aldehydes[7,10,11,17,18,29,30] and aryl isothiocynates.[23] This appears to be true for the newly discovered imidazolylacryloyls that are also attracted to the topologically complementary α-cleft instead of the βCys93 binding site, with the protein binding environment and interactions serving to stabilize the covalent adduct between the β-unsaturated carbon and the αVal1 nitrogen. The absence of such a protein stabilization effect may in part explain the non-reactivity of the compound towards free valine.

We note that even though different classes of compounds bind at the same α-cleft, they exhibit different allosteric behaviors, with the direction and magnitude of the allosteric shift depending on preferential stabilization of one state (T or R) over the other.[7,8,29,30] Thus, the slight left-shift with some of the compounds, *e.g.* KAUS-12 and KAUS-15, may mean that the stabilization effect on the R-state (most likely binding to the R2-state Hb) becomes predominant, while for KAUS-10, which slightly right-shifts the OEC, the T-state stabilization may be more dominant. These studies support the general principle that allosteric effectors can bind to the same site but produce opposite allosteric effects.

GSH plays a major cellular role in removing toxic electrophilic xenobiotics, and thus compounds with a reactive β-unsaturated carbon like KAUS could pose a toxicity risk to the cell.[51] However, unlike ECA, the KAUS compounds showed weak reactivity towards GSH. Minimal cellular toxicity was also observed for the tested compounds, KAUS-12 and KAUS-15 (IC_{50} > 1.6 mM) when compared to ECA (IC_{50} of 22 μM) with the C-166 mouse fibroblast cell line. These studies suggest that the KAUS compounds may have a more favorable therapeutic index than ECA.

Conclusion

Pharmacological stabilization of R-state Hb and/or destabilization of T-state Hb, which leads to an increase in Hb affinity for oxygen, offers a therapeutic strategy to treat SCD. We have designed a new class of Hb covalent modifiers, imidazolylacryloyl derivatives, that were envisaged to increase Hb oxygen affinity and concomitantly prevent red blood cell sickling. *In vitro* analyses showed the compounds to exhibit very weak if any left-shifting and/or antisickling activities. Crystallographic studies of the compounds complexed to deoxyHb reveal an unexpected result that showed the compounds binding not on the surface of the protein as predicted but rather inside the central water cavity, which stabilizes the T-state Hb and – paradoxically – explains their suboptimal activity. The observed mode of binding appears to be due to the increased reactivity of the β-unsaturated carbon and the highly specialized α-cleft binding pocket that attracts and maximizes interactions with the KAUS molecules, as well as provides stabilization to the covalent adduct. Nonetheless, we are encouraged by the fact that these compounds still bind in a covalent manner, which was one of our objectives, providing the framework for specific modification of the KAUS molecules to develop potent antisickling agents.

Experimental section

Materials and chemistry

Ethacrynic acid was purchased from Santa Cruz Biotechnology. Glutathione (GSH), L-cysteine, L-valine, L-histidine, L-lysine, 5,5′-dithiobis-(2-nitrobenzoic acid) (DTNB), and sulforhodamine were purchased from Sigma-Aldrich. Reagents and solvents for chemical synthesis were purchased from Sigma-Aldrich (USA), Alfa Aeser (UK) or Acros Organics (Belgium) as ACS-reagent grade and used without further purification. Anhydrous solvents were prepared according to standard methods. Solvents for LC-MS or UPLC-MS were purchased from the same vendors mentioned above and used without further purification. RPMI-1640, fetal bovine serum and other cell culture materials were purchased from Lonza Group Ltd (Basel, Switzerland). Mouse normal fibroblast cells (C-166) were a generous gift from Dr Ahmed M. Al-Abd, National Research Center, Cairo, Egypt. Cells were maintained in RPMI-1640 containing 100 U mL^{-1} penicillin, 100 μg mL^{-1} streptomycin, and 0.025 μg mL^{-1} amphotericin B, supplemented with 10% heat-inactivated fetal bovine serum (FBS). Cell lines were incubated under standard conditions in a humidified 5% (v/v) CO_2 atmosphere at 37 °C.

Compounds **1a–1i** (Fig. 1) were synthesized as described below. Except as otherwise indicated, all synthetic reactions were carried out under nitrogen atmosphere in flame- or oven-dried glassware, and solvents were freshly distilled. Tetrahydrofuran (THF) was distilled from sodium/benzophenone. Reactions were monitored by thin layer chromatography (TLC) with 0.25 mm E. Merck pre-coated silica gel plates. ^{1}H-NMR spectra

were recorded on a Bruker AV-300 NMR spectrometer with TopSpin software. Infrared spectra were recorded on a Bruker FT-IR spectrometer. Melting points were recorded on a Buchi melting point apparatus and are uncorrected. LC/MS were run on an Agilent 6130 Series, single quad.

De-identified, leftover EDTA venous blood samples from patients with SCD, who visited The Children's Hospital of Philadelphia for routine clinic visits, were obtained after informed consent. Normal whole blood was collected from adult donors at the Virginia Commonwealth University after informed consent. Hb was purified from discarded normal blood samples following a published procedure.[46] The use of these human samples is in accordance with the regulations of the IRB for Protection of Human Subjects.

Preparation of imidazolylacryloyl derivatives 1a–1i

Synthesis of 1-(2,3-dichloro-4-hydroxyphenyl)ethan-1-one (2a). A solution of 2,3-dichloroanisole (75 g, 423.68 mmol) in dichloromethane (1.5 L) was cooled to 0 °C, followed by portion-wise addition of aluminum chloride (112.98 g, 847.36 mmol), and was stirred for 10 min. Acetyl chloride (39.90 g, 508.416 mmol) was added drop-wise over a period of 25 min, and stirred at 25 to 27 °C for 30 min. The reaction mass was cooled to 0 °C and then quenched by addition of water (200 mL), and the product extracted from the aqueous phase using dichloromethane (2 × 500 mL). The combined organic layer was washed with water (200 mL) and brine (250 mL), dried over anhydrous sodium sulfate and concentrated under vacuum to obtain the crude product as an off-white solid. The crude solid was triturated with *n*-hexane (500 mL) and the solid filtered to afford the intermediate 4-acetyl-2,3-dichloroanisole as an off-white solid (61 g, 65.7%). Mp 81.8–82.6 °C; ^{1}H-NMR (300 MHz, $CDCl_3$-*d*) δ_H ppm 7.55 (d, 1H, *J* = 8.7 Hz Ar-H5), 6.9 (d, 1H, *J* = 8.7 Hz, Ar-H6) 3.98 (s, 3H, OCH_3), 2.65 (s, 3H, COH_3).

A solution of 4-acetyl-2,3-dichloroanisole (50 g, 228.31 mmol) in acetic acid (150 mL) was warmed to 60° C and added to hydrobromic acid (47% in water, 3.3 L) drop-wise over a period of 1 h. The reaction mass was heated to 100 °C for 16 h, and then cooled to about 0° C, followed by quenching with water (1 L). The product was extracted from the aqueous phase using dichloromethane (2 × 1 L). The organic layer was dried over anhydrous sodium sulfate and concentrated under vacuum to obtain a yellow solid. The crude product was dissolved in 10% aqueous sodium hydroxide solution (500 mL), and the aqueous layer washed with ethyl acetate (2 × 250 mL). The aqueous layer, which was maintained between 0 and 5 °C, was acidified with HCl (1.5 N, 750 mL), and the product extracted using dichloromethane (2 × 500 mL). The combined organic layer was washed with water (500 mL) followed by brine (500 mL), dried over anhydrous sodium sulfate, and concentrated under vacuum to afford **2a** as a white solid (10 g, 21.3%), mp 151.2–153.5 °C. ^{1}H NMR (300 MHz, $CDCl_3$) δ_H ppm 7.55 (d, 1H, *J* = 8.7 Hz Ar-H5), 7.03 (d, 1H, *J* = 8.7 Hz, Ar-H6), 6.03 (br, 1H, OH), 2.66 (s, 3H, $COCH_3$). LC/MS (ESI) *m*/*z* = 205 (M + 1), purity = 95.8%.

Synthesis of 2-(4-acetyl-2,3-dichlorophenoxy)acetic acid (4a). A solution of 2,3-dichloro-4-hydroxyacetophenone **2a** (3.5 g, 17.073 mmol) in *N*,*N*-dimethylformamide (DMF) (35 mL) was cooled to 0 °C, followed by addition of potassium carbonate (7.09 g, 51.219 mmol). The mixture was stirred at 25 to 27 °C for 15 min and ethyl bromoacetate (3.4 g, 20.48 mmol) was added drop-wise over a period of 15 min. The reaction mass was heated to 80 °C and stirred at the same temperature for 2 h, then cooled to room temperature and quenched with water (100 mL). The product was extracted from the aqueous phase using methyl *tert*-butyl ether (MeOtB) (2 × 100 mL). The combined organic layer was washed with water (100 mL) and brine (100 mL), dried over anhydrous sodium sulfate, and concentrated under vacuum to afford **3a** as a pale yellow liquid (4.97 g, 100%). The crude product was taken into the next step without further purification. ^{1}H NMR ($CDCl_3$) δ_H ppm 7.50 (d, 1H, *J* = 8.7 Hz, Ar-H5), 6.79 (d. 1H, *J* = 8.7 Hz, Ar-H6), 4.78 (s, 2H, OCH_2), 4.29 (q, 2H, *J* = 6.9 Hz, CH_2), 2.66 (d, 3H, $COCH_3$). 1.32 (t, 3H, *J* = 6.9 Hz, CH_3). MS (ESI) *m*/*z* = 202.9 (M − $CH_2COOCH_2CH_3$), 205, 207.

A solution of **3a** (1.8 g, 6.18 mmol) in tetrahydrofuran (THF) (7.2 mL) was cooled to 0 °C and lithium hydroxide (1.29 g, 30.91 mmol) in water (1.8 mL) was added. The reaction mixture was stirred at 25 to 27 °C for 5 h, and then acidified with aqueous 1.5 N hydrochloric acid (25 mL). The product was extracted from the aqueous phase using dichloromethane (2 × 25 mL). The organic layer was dried using anhydrous sodium sulfate, and concentrated under vacuum to obtain a brown solid. The crude solid was basified with 10% aqueous sodium bicarbonate (20 mL), the aqueous layer washed with ethyl acetate (EtOAC) (25 mL), then cooled to 4 °C and acidified using aqueous 1.5 N hydrochloric acid (HCl) (50 mL). The product was extracted from the aqueous phase using dichloromethane (DCM) (2 × 25 mL). The organic layer was washed with water (50 mL) and brine (50 mL), dried over anhydrous sodium sulfate and concentrated under vacuum to give **4a** as a pale brown solid (1.5 g, 94.33%), mp 150.6–153.5 °C. ^{1}H NMR (300 MHz, DMSO-d_6) δ_H ppm 13.3 (br s, 1H, OH), 7.72 (d, 2H, *J* = 8.4 Hz, Ar-H5), 7.16 (d, 2H, *J* = 9 Hz, Ar-H6), 4.96 (s. 2H, CH_2), 2.57 (s, 3H, CH_3). LC/MS (ESI) *m*/*z* = 261 (M − 1), 263 (M +), 245 (M + 2), purity = 99.55%.

Synthesis of 4-(4-acetyl-2,3-dichlorophenoxy)butanoate (4c). A solution of 2,3-dichloro-4-methoxyacetophenone (4.5 g, 21.95 mmol) in DMF (45 mL) was cooled to 0 °C, then potassium carbonate (9.08 g, 65.85 mmol) added, and the mixture was stirred at 25 to 27 °C for 15 min. Ethyl 4-bromobutyrate (5.141 g, 26.34 mmol) was added drop-wise over a period of 15 min, and then the mixture heated to 80 °C for 2 h. The reaction mass was cooled to ambient temperature and quenched with water (100 mL). The product was extracted from the aqueous phase using MeOtB (2 × 100 mL). The combined organic layer was washed with water (100 mL), followed by brine (100 mL). The organic layer was dried over anhydrous sodium sulfate and concentrated under vacuum to get a pale yellow liquid. The crude material was purified by column chromatography over silica gel (230–400 mesh) using 40 to

50% ethyl acetate in hexane as eluent to afford **3c** as a pale brown liquid (3.8 g, 58.4%). ^{1}H NMR (300 MHz, DMSO-d_6) δ_H 7.52 (d, 1H, J = 9.3 Hz, Ar-H5), 6.89 (d. 1H, J = 10.8 Hz, Ar-H6), 4.20–4.13 (m, 4H, two OCH_2), 2.65 (s, 3H, $COCH_2$), 2.57 (d, 2H, $COCH_2$), 2.19 (q, 2H, J = 6.3 Hz, CH_2), 1.28 (t, 3H, J = 6.9, 7.2 Hz, CH_3); LC/MS (ESI) m/z = 319 (M + 1), 321 (M + 3), 323 (M + 5), purity = 99.13%.

A solution of 4-(4-acetyl-2,3-dichlorophenoxy)butyric acid ethyl ester **3c** (3.4 g, 10.65 mmol) in THF (13.6 mL) was cooled to 0 °C and 3.4 mL lithium hydroxide (2.23 g, 53.26 mmol) was added. The above suspension was stirred at 25 to 27 °C for 4 h, and the reaction mass cooled to 0 °C and quenched with 1.5 N hydrochloric acid (25 mL). The product was extracted from the aqueous phase using DCM (2 × 50 mL). The combined organic layer was washed with water (50 mL) and brine (25 mL). The organic layer was dried over anhydrous sodium sulfate, and concentrated under vacuum to obtain an off-white solid. The crude product was dissolved in 10% sodium bicarbonate (25 mL) and the aqueous layer washed with EtOAc (50 mL), cooled and acidified with 1.5 N HCl (50 mL). The product was extracted from the aqueous phase using DCM (2 × 50 mL), and the combined organic layer washed with water (50 mL) and brine (25 mL). The organic layer was dried over anhydrous sodium sulfate and concentrated under vacuum to afford **4c** as a white solid (2.6 g, 76.47%), mp 151.2–154.6 °C. ^{1}H NMR (300 MHz, DMSO-d_6) δ_H ppm 1.94–2.05 (m, 2H) 2.39–2.48 (m, 3H) 2.57 (d, J = 1.89 Hz, 4 H) 4.20 (t, J = 6.33 Hz, 2H) 7.25 (dd, J = 8.78, 1.61 Hz, 1H) 7.74 (dd, J = 8.69, 1.70 Hz, 1H) 12.20 (br s, 1H); LC/MS (ESI) m/z = 203 (M − $(CH_2)_3COOH$), 205, 207, purity = 96.94%.

Synthesis of 2-(4-acetyl-2-chlorophenoxy) acetic acid (4d). This compound was prepared following the procedure detailed above for the synthesis of the similar analogue **4a**. The crude product was purified by acid–base workup to afford **4d** as an off-white solid (5.5 g, 82.0%), mp 147.8–149.2 °C. ^{1}H NMR (300 MHz, DMSO-d_6) δ_H 13.24 (s, 1H, OH), 7.99 (d, 1H, J = 2.1 Hz Ar-H3), 7.89 (r, 1H, J = 6.6, 2.1 Hz, Ar-H5), 7.15 (d, 1H, J = 8.7 Hz, Ar-H6), 4.94 (s. 2H, OCH_2), 2.51 (under DMSO, $COCH_3$); LC/MS (ESI) m/z = 227 (M − 1), 229 (M + 1); purity = 99.43%.

Synthesis of 4-(4-acetyl-2-chlorophenoxy)butyric acid (4f). This compound was prepared following the procedure described above for the synthesis of the similar analogue **4c** and was obtained as an off-white solid (5.5 g, 82.08%), mp 129.2–135.8 °C. ^{1}H NMR (300 MHz, DMSO-d_6) δ_H ppm 12.38 (br s, 1H, OH), 7.98–7.25 (m, 2H, Ar-H3, 5), 7.26 (d, 1H, J = 8.7 Hz, Ar-H6), 4.19 (t, 2H, J = 6.3 Hz, OCH_2), 2.54–2.41 (m, 5H, CH_3 & CH_2), 1.99 (t, 2H, J = 6.3, 6.9 Hz, CH_2); LC/MS (ESI) m/z = 169 (M − $(CH_2)_3COOH$), purity = 97.71%.

Synthesis of ethyl 2-(4-acetyl-3-chlorophenoxy) acetic acid (4g). This compound was prepared following the procedure described above for the synthesis of the similar analogue **4a** and was obtained as an off-white solid (5.5 g, 82.08%), mp 103.7–106.5 °C. ^{1}H NMR (300 MHz, DMSO-d_6) δ_H 13.18 (s, 1H, OH), 7.77 (d, 1H, J = 8.7 Hz, Ar-H5), 7.10 (d, 1H, J = 2.7 Hz, Ar-H2), 7.02 (s, 1H, Ar-H6), 4.83 (s, 2H, OCH_2), 2.51 (under DMSO, $COCH_3$); LC/MS (ESI) m/z = 227 (M − 1), 229 (M + 1); purity = 99.45%.

Synthesis of 4-(4-acetyl-3-chlorophenoxy)butanoic acid (4i). This compound was prepared following the procedure described above for the synthesis of the similar analogue **4c** and was obtained as an off-white solid (5.5 g, 73.3%), mp 105.9–109.0 °C. ^{1}H NMR (300 MHz, DMSO-d_6) δ_H 12.2 (br s, 1H, OH), 7.75 (d, 1H, J = 8.7 Hz, Ar-H5), 7.10 (d, 1H, J = 2.4 Hz, Ar-H2), 7.01 (q, 1H, J = 2.4, 8.7 Hz, Ar-H6), 4.09 (t, 2H, J = 6.6, 6.3 Hz, OCH_2), 2.50 (under DMSO, $COCH_3$), 2.38 (t, 2H, J = 7.5, 7.2 Hz, CH_2), 1.49 (t, 2H, J = 6.6, 6.9 Hz, CH_2); IR (FT-IR, cm^{-1}): 2914.9, 1668.2, 1614.4, 1591.6, 1564.7, 1473.6, 1409.5, 1373.4, 1257.9; LC/MS (ESI) m/z = 196 (M − $(CH_2)_3COOH$), 171; purity = 98.94%.

Synthesis of 1-(triphenylmethyl)-1*H*-imidazole-2-carbaldehyde (5). Sodium hydride (7.4 g, 312.29 mmol) in DMF (125 mL, 5 vol.) was cooled to 0 °C, 2-imidazolecarboxaldehyde (25 g, 260.19 mmol) was added portion-wise, and the reaction mass was stirred at 28 °C for 30 min. The reaction mass was cooled to 0 °C followed by drop-wise addition of a solution of trityl chloride (87 g, 312.29 mmol) in DMF (175 mL) and was stirred for 1 h under the same cooling conditions until completion (TLC monitoring). The reaction mixture was quenched with ammonium chloride solution (500 mL), and extracted with MeOtB (250 mL). The organic layer was dried over sodium sulfate, and the solvent removed under reduced pressure to obtain the crude product, which was purified by column chromatography over neutral alumina by using 0 to 7% ethyl acetate in hexane as eluent. The product 1-(triphenylmethyl)-1*H*-imidazole-2-carbaldehyde was a white solid (33 g, 37%), mp 165.9–160.7 °C. ^{1}H NMR (300 MHz, DMSO-d_6) δ_H ppm 6.97–7.14 (m, 9H) 7.32–7.49 (m, 13H) 9.14 (s, 1H). LC/MS (ESI) m/z = 337 (M − 1), purity = 86.79%.

Synthesis of {2,3-dichloro-4-[(*E*)-3-1*H*-imidazol-2-ylacryloyl]-phenoxy}acetic acid (1a). 1-Trityl-1*H*-imidazole-2-carbaldehyde **5** (2.89 g, 8.55 mmol) and acetophenone derivative **4a** (1.5 g, 5.7 mmol) were dissolved in ethanol (51 mL). The reaction mixture was cooled to 0 °C and 1 N aqueous NaOH solution (51.75 mL) was added drop-wise over a period of 30 min while keeping the temperature between 0 to 5 °C. The mixture was then stirred at 25 to 27 °C for 48 h, followed by dilution with water (50 mL). The aqueous layer was washed with MeOtB (2 × 200 mL), cooled to 0 to 5 °C, and 1.5 N HCl (50 mL) added drop-wise to adjust the pH to 4. The solid formed was filtered and dried under vacuum to afford a pale yellow solid of **6a**. The crude product was taken into the next step without further purification (2.5 g, 75.75%).

A solution of **6a** (2.5 g, 4.284 mmol) in DCM (12.5 mL) was cooled 0° C and trifluoroacetic acid (5 mL) in DCM (12.5 mL) added drop-wise over a period of 15 min. The reaction mass was stirred at 25 to 27 °C for 1 h, then concentrated under vacuum to afford a yellow solid. To the crude solid, MeOtB (100 mL) was added, stirred at 25 to 27 °C for 15 min, filtered and dried under vacuum to afford a yellow solid. Water (20 mL) was added to the crude product and cooled to 0 °C and basified with 5% sodium hydroxide solution (10 mL) to

pH 9. The suspension was stirred at 25 to 27 °C for 15 min, and then cooled and acidified using 1.5 N HCl (20 mL) until the pH was adjusted to 4. The solid was filtered and dried under vacuum to afford **1a** as a pale yellow solid product (1 g, 71.42%), mp 273.0–274.1 °C. ^{1}H NMR (300 MHz, DMSO-d_6) δ_H 12.70 (br, 2H, NH & OH), 7.53 (d, 1H, J = 9.3 Hz, Ar-H5), 7.33–7.12 (m, 5H, Ar-H6 & imidazole-H & 2CH), 4.98 (s, 2H, CH_2); LC/MS (ESI) m/z = 339 (M − 1), 341 (M + 1), 343 (M + 3), purity = 98.08%. Anal. Calcd for ($C_{14}H_{10}Cl_2N_2O_4$): C, 49.29; H, 2.95; Cl, 20.78; N, 8.21. Found C, 49.17; H, 2.96; Cl, 20.74; N, 8.18.

Synthesis of 4-{2,3-dichloro-4-[(2*E*)-3-(1*H*-imidazol-2-yl)prop-2-enoyl]phenoxy}butanoic acid (1c). To a cooled solution of 1-(triphenylmethyl)-1*H*-imidazole-2-carbaldehyde **5** (2.6 g, 7.72 mmol) and 4-(4-acetyl-2,3-dichloro-phenoxy)-butyric acid **4c** (1.5 g, 1.51 mmol) in ethanol (51.7 mL) at 0 to 5° C, 1 N NaOH solution (52 mL) was added drop-wise over a period of 15 min. The reaction mass was stirred at 25 to 27° C for 24 h while monitoring by TLC. The reaction mass was diluted with water (10 mL), washed with MeOtB (25 mL), and cooled to 0 to 5 °C. HCl (1.5 N, 5 mL) added drop-wise to adjust the pH to 4. The solid formed was filtered and dried under vacuum to afford **6c** a pale yellow solid.

The crude **6c** (2.8 g, 4.59 mmol) was dissolved in DCM (14 mL), cooled to 0 °C, and trifluroacetic acid (5.6 mL) in DCM (14 mL) added drop-wise while keeping the temperature between 0 to 5 °C. The reaction mass was allowed to stir at 25 to 27 °C for 1 h. The solvent was removed under reduced pressure and the crude solid was triturated with MeOtB (20 mL), filtered and dried to afford the product as a yellow solid (1.2 g, 75.0%), mp 214.9–217.2 °C; ^{1}H NMR (300 MHz, DMSO-d_6) δ_H 12.98 (br, 1H, OH), 12.22 (s, 1H, NH), 7.33–7.13 (m, 5H, Ar-H & imidazole-H & 2CH), 4.21 (t, 2H, J = 5.7 Hz, OCH_2), 2.45 (under DMSO, CH_2), 2.01 (t, 2H, J = 6.3 Hz, CH_2); IR (FT-IR, cm^{-1}): 2938.8, 1681.1, 1609.7, 1584.6, 1446.0, 1387.6, 1303.0; LC/MS (ESI) m/z = 367 (M − $(CH_2)_3$COOH), 369, 371; purity = 99.76%. Anal. Calcd for ($C_{16}H_{12}Cl_4N_2O_4$): C, 43.87; H, 2.76; Cl, 32.37; N, 6.39. Found: C, 43.76; H, 2.75; Cl, 32.44; N, 6.38.

Synthesis of 2-{2-chloro-4-[(2*E*)-3-(1*H*-imidazol-2-yl)prop-2-enoyl]phenoxy}acetic acid (1d). This compound was prepared according to the procedure described for the preparation of the similar analogue **1a** and was obtained as a yellow solid (1 g , 76%), mp 246.9–248.7 °C; ^{1}H NMR (300 MHz, DMSO-d_6) δ 8.01 (s, 1H, Ar-H3), 7.93(t, 2H, J = 6, 10.5 Hz, CH & Ar-H5), 7.45 (d, 1H, J = 15.6 Hz, CH), 7.28 (s, 2H, imidazole-H), 7.07 (d, 1H, J = 8.7 Hz, Ar-H6), 4.59 (s, 2H, OCH_2); IR (FT-IR, cm^{-1}): 3143.8, 2918.5, 1670.3, 1588.0, 1483.0, 1409.9, 1259.2, 1238.7; LC/MS (ESI) m/z = 307 (M − 1), 307 (M + 1), purity = 97.92%. Anal. Calcd for ($C_{16}H_{12}Cl_4N_2O_4$): C, 43.87; H, 2.76; Cl, 32.37; N, 6.39. Found: C, 43.76; H, 2.75; Cl, 32.44; N, 6.38.

Synthesis of 4-{2-chloro-4-[(2*E*)-3-(1*H*-imidazol-2-yl)prop-2-enoyl]phenoxy}butanoic acid (1f). This compound was prepared according to the procedure described for the preparation of the similar analogue **1c** and was obtained as a pale yellow solid (1.2 g, 68.95%), mp 210.2–214.2 °C; ^{1}H NMR (300 MHz, DMSO-d_6) δ_H 12.84 (br, 1H, OH), 12.23 (s, 1H, NH), 8.10 (s, 1H, Ar-H3), 8.04(d, 1H, J = 9 Hz, Ar-H5), 7.89 (d, 1H, J = 15.6 Hz, CH), 7.48 (d, 1H, J = 15.6 Hz, CH), 7.37–7.35 (m, 3H, Ar-H6 & imidazole-H), 4.22 (t. 2H, OCH_2), 2.45 (under DMSO, CH_2), 2.01 (t, 2H, CH_2). LC/MS (ESI) m/z = 333 (M − 1), 335 (M + 1), purity = 97.62%. Anal. Calcd for ($C_{16}H_{15}ClN_2O_4$): C, 57.41; H, 4.52; Cl, 10.59; N, 8.37. Found C, 57.46; H, 4.50; Cl, 10.55; N, 8.34.

Synthesis of 2-{3-chloro-4-[(2*E*)-3-(1*H*-imidazol-2-yl)prop-2-enoyl]phenoxy}acetic acid (1g). This compound was prepared according to the procedure described for the preparation of the similar analogue **1a** and was obtained as a yellow solid (1.2 g, 75.08%), mp 258.3 °C; ^{1}H NMR (300 MHz, DMSO-d_6) δ_H 13.02 (br, 1H, NH), 7.57 (d, 1H, J = 8.4 Hz, Ar-H5), 7.31–7.15 (m, 5H, Ar-H2 & imidazole-H & 2CH), 7.05 (d, 1H, J = 8.4 Hz, Ar-H6), 4.85 (s, 2H, OCH_2); IR (FT-IR, cm^{-1}): 3142.3, 1672.7, 1590.8, 1553.46, 1413.3, 1329.8, 1251.4, 1222.7; LC/MS (ESI) m/z = 307 (M + 1), 309 (M + 3); purity = 98.19%. Anal. Calcd for ($C_{14}H_{11}ClN_2O_4$): C, 54.83; H, 3.62; Cl, 11.56; N, 9.13. Found C, 54.72; H, 3.63; Cl, 11.58; N, 9.14.

Synthesis of 4-{3-chloro-4-[(2*E*)-3-(1*H*-imidazol-2-yl)prop-2-enoyl]phenoxy}butanoic acid (1i). This compound was prepared according to the procedure described for the preparation of the similar analogue **1c** and was obtained as a yellow solid (2.2 g, 73.08%), mp 219.4–222.8 °C. ^{1}H NMR (300 MHz, DMSO-d_6) δ_H 12.23 (br, 1H, OH), 7.59 (d, 1H, J = 8.7 Hz, Ar-H5), 7.36–7.17(m, 5H, 2CH, 2imidazole-H & Ar-H), 7.06 (d, 1H, J = 8.7 Hz, Ar-H6), 4.11 (t, 2H, J = 6, 6.3 Hz, OCH_2), 2.40 (t, 2H, J = 7.2 Hz, CH_2), 1.79 (q, 2H, CH_2); IR (FT-IR, cm^{-1}): 3236.0, 1695.8, 1660.8, 1585.6, 1550.6, 1444.8, 1345.6, 1321.3, 1296.6; LC/MS (ESI) m/z = 335 (M + 1) and 337 (M + 3), purity = 98.74%.

Synthesis of 1-[2,3-dichloro-4-(2-[1,3]dioxolan-2-yl-ethoxy)-phenyl]ethanone (7a). A solution of 2,3-dichloro-4-methoxy-acetophenone (5.5 g, 26.82 mmol) in DMF (55 mL) was cooled to 0 to 5 °C, potassium carbonate (11.12 g, 80.51 mmol) added, and the mixture stirred at 25 to 27 °C for 15 min. 2-(2-Bromoethyl)-1,3-dioxalane (5.82 g, 32.19 mmol) was added to the above suspension drop-wise over a period of 15 min. The reaction mass was heated to 80 °C and maintained at the same temperature for 2 h, followed by cooling to ambient temperature and quenching with water (100 mL). The product was extracted from the aqueous phase using MeOtB (2 × 100 mL), and the combined organic layer washed with water (100 mL) and brine (100 mL), dried over anhydrous sodium sulfate and concentrated under vacuum to obtain a pale brown gum. Hexane (70 mL) was added to the residue and the suspension stirred at 25 to 27° C for 30 min, filtered and dried under vacuum to obtain **7a** as a brown solid (6.8 g, 84.69%). ^{1}H NMR (300 MHz, $CDCl_3$) δ_H ppm 7.53 (m, J = 8.88 Hz, 2H), 7.28 (s, 1H), 6.91 (m, J = 8.69 Hz, 2H), 5.16 (t, J = 4.72 Hz, 2H), 4.26 (t, J = 6.52 Hz, 5H), 3.85–4.08 (m, 10H),), 2.65 (s, 7H), 2.25 (td, J = 6.47, 4.82 Hz, 5H).

Synthesis of 1-{3-chloro-4-[2-(1,3-dioxolan-2-yl)ethoxy]-phenyl}ethanone (7b). This compound was prepared according to the procedure described above for the preparation of **7a**.

The crude product, obtained as an off-white solid (7.9 g, 100%), was used for the next step without further purification. ^{1}H NMR (300 MHz, $CDCl_3$) δ_H ppm 8.00 (1H, d, J = 1.89 Hz), 7.86 (1H, dd, J = 8.59, 1.98 Hz), 6.98 (1H, d, J = 8.69 Hz), 5.17 (1H, t, J = 4.82 Hz), 4.28 (2H, t, J = 6.52 Hz), 3.78–4.08 (4H, m), 2.57 (3H, s), 2.36–2.16 (2H, m), 1.65 (1H, br s). LC/MS (ESI) m/z = 271 (M + 1), purity = 95.46%.

Synthesis of 1-{2-chloro-4-[2-(1,3-dioxolan-2-yl)ethoxy]-phenyl}ethanone (7c). This compound was prepared according to the procedure described above for the preparation of **7a**. The crude product was obtained as a pale brown liquid (7.9 g, 100%) and used for the next step without further purification. ^{1}H NMR (300 MHz, $CDCl_3$) δ_H ppm 7.68 (1H, d, J = 8.50 Hz), 6.96 (1H, br s), 6.85 (1H, d, J = 8.50 Hz), 5.13–4.95 (1H, m), 4.2–4.10 (1H, m), 3.76–4.10 (5H, m), 3.39–3.54 (1H, m), 2.65 (2H, s), 2.29–2.07 (2H, m). LC/MS (ESI) m/z = 271 (M + 1), purity = 93.88%.

Synthesis of 3-(4-acetyl-2,3-dichlorophenoxy)propionic acid (8a). To a solution of **7a** (6.8 g, 22.84 mmol) in acetone (68 mL) was added 1.5 N HCl (68 mL) drop-wise at 0 to 5 °C over a period of 20 min. The reaction mixture was stirred at 25 to 27 °C for 16 h, and then concentrated under vacuum. The crude product was diluted with water (50 mL) and extracted with DCM (2 × 50 mL). The combined organic layer was washed with water (50 mL) and brine (50 mL), dried over anhydrous sodium sulfate, and concentrated under vacuum to give a pale yellow gum. The above material was dissolved in DMF (58 mL), oxone (7.012 g, 22.841 mmol) was added, and the mixture stirred at 25 to 27° C for 6 h. The reaction mass was diluted with water (50 mL) and the product extracted from the aqueous layer using dichloromethane (2 × 100 mL). The combined organic layer was dried over anhydrous sodium sulfate, and concentrated under vacuum to yield a pale brown gum. The crude solid was dissolved in ethyl acetate (100 mL) and washed with 10% sodium bicarbonate (75 mL). The aqueous layer was cooled to 5 °C and acidified using 1.5 N HCl (50 mL) to a pH of 3. The product was extracted from the aqueous phase using MeOtB (2 × 250 mL). The combined organic layer was washed with water (2 × 250 mL) and brine (100 mL), dried over anhydrous sodium sulfate, and concentrated under vacuum to give **8a** as an off-white solid product (2.9 g, 47%), mp 142.2–144.9 °C. ^{1}H NMR (300 MHz, DMSO-d_6) δ_H ppm 7.75 (1H, d, J = 8.88 Hz), 7.29 (1H, d, J = 8.69 Hz), 4.36 (2H, t, J = 5.85 Hz), 2.77 (2H, t, J = 5.76 Hz), 2.58 (3H, s). LC/MS (ESI) m/z = 203 (M − $(CH_2)_2$COOH), 205, 207, purity = 100%.

Synthesis of 3-(4-acetyl-2-chlorophenoxy)propionic acid (8b). This compound was prepared according to the procedure described above for the preparation of **8a**. The product was obtained as an off-white solid (3 g, 49.18%), mp 124.7–127.9 °C. ^{1}H NMR (300 MHz, DMSO-d_6) δ_H ppm 7.85–8.02 (2H, m), 7.30 (1H, d, J = 8.50 Hz),4.35 (2H, t, J = 5.85 Hz), 3.34 (1H, br s), 2.64–2.84 (2H, m), 2.54 (2H, s); LC/MS (ESI) m/z = 169 (M − $(CH_2)_2$COOH), 171, purity = 97.85%.

Synthesis of 3-(4-acetyl-3-chlorophenoxy)propionic acid (8c). This compound was prepared according to the procedure described above for the preparation of **8a**. The product was obtained as an off-white solid (3.2 g, 45.13%), mp 95.9–98.2 °C. ^{1}H NMR (300 MHz, methanol-d_4) δ ppm 12.44 (1H, br s), 7.77 (1H, d, J = 8.50 Hz), 6.90–7.16 (1H, m), 4.26 (1H, t, J = 5.85 Hz), 3.33 (1H, s), 2.71 (1H, t, J = 5.67 Hz), 2.52 (4H, d, J = 15.30 Hz). LC/MS (ESI) m/z = 169 (M − $(CH_2)_2$COOH), 171, purity = 93.54%.

Synthesis of 3-{2,3-dichloro-4-[(2*E*)-3-(1*H*-imidazol-2-yl)prop-2-enoyl]phenoxy}propionic acid (1b). 1 N NaOH solution (93.15 mL) was added drop-wise to a cooled solution of 1-(triphenylmethyl)-1*H*-imidazole-2-carbaldehyde (5.2 g, 15.5 mmol) **5** and **8a** (2.7 g, 9.72 mmol) in ethanol (93 mL) at 0 to 5 °C. The reaction mass was stirred at 25 to 27 °C for 24 h, and monitored by TLC. After completion of the reaction, the mixture was diluted with water (10 mL), and the aqueous layer was washed with MeOtB (30 mL). The aqueous layer was cooled to 0 to 5 °C and 1.5 N HCl was added drop-wise to adjust the pH to 4. The solid formed was filtered and dried under vacuum to afford **9a** as a pale yellow solid.

The crude intermediate **9a** was dissolved in DCM (25 mL), cooled to 0 °C, trifluroacetic acid (10 mL, 2 vol.) in dichloromethane (25 mL) added at 0 to 5 °C and the reaction allowed to stir at 25 to 27 °C for 1 h. The solvent was removed under reduced pressure, and the crude solid triturated with MeOtB (50 mL), filtered and dried under vacuum to afford the crude product as a yellow solid. The solid was suspended in water (40 mL), and the pH adjusted to 9 using 5% aqueous NaOH solution at 0 to 5 °C. The reaction mass was allowed to stir at 25 to 27 °C for 15 min, and then acidified to pH 4 using 1.5 N HCl. The crude product was further purified by crystallization from DMF–acetonitrile mixture to afford **1b** as a yellow solid (0.8 g, 23.52%), mp 223.2–226.6 °C. ^{1}H NMR (300 MHz, DMSO-d_6) δ_H ppm 7.56 (1H, d, J = 8.69 Hz), 7.28–7.45 (3H, m), 7.06–7.28 (2H, m), 4.38 (2H, t, J = 5.76 Hz), 2.70–2.85 (2H, m); IR (FT-IR, cm^{-1}): 3261.2, 1692.1, 1669.3, 1605.8, 1581.9, 1547.7, 1388.7, 1302.7, 1249.4; LC/MS (ESI) m/z = 283 (M − $(CH_2)_2$COOH), 285, 287; purity = 95.97%. Anal. Calcd for ($C_{15}H_{12}Cl_2N_2O_4$): C, 50.72; H, 3.41; Cl, 19.96; N, 7.89. Found C, 50.63; H, 3.40; Cl, 19.92; N, 7.87.

Synthesis of 3-{2-chloro-4-[(*E*)-3-(1*H*-imidazol-2-yl)acryloyl]-phenoxy}propionic acid (1e). This compound was prepared according to the procedure described above for the preparation of **1b** and was obtained as a yellow solid (0.53 g, 16.6%), mp 220–223.5 °C. ^{1}H NMR (300 MHz, DMSO-d_6) δ_H ppm 12.49 (1H, br s), 7.99–8.14 (2H, m), 7.89 (1H, d, J = 15.67 Hz), 7.26–7.55 (4H, m), 4.39 (2H, t, J = 5.76 Hz), 2.80 (2H, t, J = 5.76 Hz); IR (FT-IR, cm^{-1}): 3258.2, 1708.7, 1671.6, 1660.5, 1607.9, 1590.2, 1503.1, 1412.5, 1260.9, 1207.0; LC/MS (ESI) m/z = 247 (M − $(CH_2)_2$COOH), 249, purity = 96.13%. Anal. Calcd for ($C_{15}H_{13}ClN_2O_4$): C, 56.17; H, 4.09; Cl, 11.05; N, 8.73. Found C, 56.03; H, 4.10; Cl, 11.07; N, 8.75.

Synthesis of 3-{3-chloro-4-[(*E*)-3-(1*H*-imidazol-2-yl)acryloyl]-phenoxy}propionic acid (1h). This compound was prepared according to the procedure described above for the preparation of **1b** and was obtained as a yellow solid (1.2 g, 70%), mp 237.3–238.2 °C; ^{1}H NMR (300 MHz, DMSO-d_6) δ_H ppm, 7.57 (1H, d, J = 8.50 Hz), 7.12–7.44 (5H, m), 7.07 (1H, d, J = 8.50

Hz), 4.28 (2H, t, J = 5.57 Hz), 2.74 (2H, t, J = 5.57 Hz); IR (FT-IR, cm^{-1}): 3255.0, 1696.1, 1667.7, 1599.3, 1449.0 1329.6, 1305.2, 1246.73, 1246.7, 1223.7; LC/MS (ESI) m/z = 247 (M − $(CH_2)_2COOH$), 249, purity = 98.2%.

Biological evaluation

Oxygen equilibrium curve studies. The ability of the nine KAUS compounds (Fig. 1; Table 1) to left-shift the OEC (stabilize the R-state or increase the oxygen affinity of Hb) in normal whole blood was determined using multipoint tonometry as previously reported.[18] Stock solutions of all compounds were made at 250 mM or 125 mM concentration in DMSO. Blood (hematocrit of 22%) was incubated with the compound at 37 °C for 1.5 h. OEC studies were performed in duplicate at 2 mM final test compound concentrations. Ethacrynic acid (ECA) was used as the positive control.

RBC morphological antisickling studies. Six compounds, including KAUS-12, KAUS-13, KAUS-15, KAUS-16, KAUS-17, and the positive control ECA, were tested for their antisickling potencies using SS cells that had been pre-incubated with 4% O_2, as previously reported.[11,18] Briefly, SS cells were suspended in Hemox buffer (TCS Scientific Corp, Southampton, PA), pH 7.4, that contained 10 mM glucose and 0.2% bovine serum albumin. The solution was incubated under air in the absence (control) or presence of a 2 mM concentration of test compound at 37 °C for 1 h. Following this, the suspension was incubated under hypoxic conditions (4% oxygen/96% nitrogen) at 37 °C for 5 h. The suspension was fixed with 2% glutaraldehyde solution without exposure to air and then subjected to microscopic morphological analysis as previously reported.[11,18]

X-ray crystallography

Co-crystallization of deoxygenated Hb or carbonmonoxy Hb with KAUS compounds. A freshly prepared solution of KAUS-12 or KAUS-15 in DMSO was either directly incubated with deoxyHb (50 mg mL^{-1}) for 1 h or incubated with oxyHb for 1 h (followed by deoxygenation to obtain the deoxyHb-drug complex) at a Hb tetramer–compound molar ratio of 1 : 5 at 37 °C, and then crystallized with 3.2 M sulfate/phosphate precipitant, pH 6.8, using the batch method as previously described, to obtain T-state crystals in about 4 days.[11,18,22,46] The crystals obtained by first incubating the compounds with oxyHb followed by deoxygenation were poorly formed, resulting in unusable diffraction data for structure determination, while crystals obtained from directly incubating the compounds with deoxyHb diffracted to 1.7 and 1.9 Å for KAUS-12 and KAUS-15, respectively. The two crystals are isomorphous with each other, crystallizing in the space group $P2_1$ with typical cell constants of 60, 80, 53 Å, and 98°. Diffraction data statistics are shown in Table 4.

The compound–Hb complexes were also crystallized in the classical R-state form using COHb, following a previously described procedure.[18,22,46] Briefly, a solution of KAUS-12 or KAUS-15 in DMSO was incubated with oxyHb for 1 h at 37 °C at a Hb tetramer : compound molar ratio of 1 : 5. The mixture was then saturated with CO to generate COHb, and then crystallized with 3.0–3.4 M sodium monobasic phosphate and potassium phosphate dibasic, at pH values ranging from 6.4 to 7.2. One or two drops of toluene was added to the solution in each tube to facilitate crystallization. X-ray-quality crystals grew in 2–3 days as trigonal bipyrimidal crystals in the space group $P4_12_12$ with typical cell constants of 53, 53, 193 Å. The crystals diffracted to 2.8 and 2.0 Å for KAUS-12 and KAUS-15, respectively.

Diffraction data for all crystals were obtained at ~100 K on an R-axis IV++ image plate detector using CuKα X-rays (λ = 1.5417) from a Rigaku Micro-Max™-007 X-ray source equipped with Varimax confocal optics operating at 40 kV and 20 mA (Rigaku, The Woodlands, TX). Crystals were cryoprotected in their mother liquor supplemented with 15–25% glycerol. The data set was processed and scaled with Rigaku D*TREK software and the CCP4 suite of programs.[52]

Structure determination of deoxyHb in complex with KAUS-12 or KAUS-15. The two deoxyHb structures in complex with KAUS-12 and KAUS-15 were refined independently using the isomorphous T-state native deoxyHb structure (PDB code 2DN2). Cycles of refinement with COOT and CNS.[53,54] identified two-symmetry-related bound compounds at the α-cleft that appeared to form a covalent interaction with the N-terminal αVal1 nitrogens of the Hb. For both complexes, symmetry-related molecules were built into the model at the two α-subunits. Several water molecules and sulfate molecules were added and the structures refined to final R_{factor}/R_{free} of 18.2/20.6% and 21.3/24.8% for KAUS-12 and KAUS-15, respectively. The two KAUS-12 and KAUS-15 coordinates have been deposited at the PDB with accession codes of 4ROL and 4ROM, respectively.

Structure determination of COHb in complex with KAUS-12 or KAUS-15. The isomorphous α1β1 dimer classical R-state structure (1LJW) was used as the starting model to refine the KAUS-12 and KAUS-15 complexes. Unlike the T-state crystals, repeated refinements with model building and addition of water showed no observable effector binding, and as a result the two structures were not refined to conclusion. The 2.0 Å structure of KAUS-15 was refined to R_{factor}/R_{free} of 23.5/26.3, while the lower resolution 2.8 Å structure of KAUS-12 was refined to 26.4/33.5, and the refinement terminated.

Reactivity of KAUS toward glutathione (GSH) and the free amino acids L-Cys, L-Val, L-His and L-Lys. A freshly prepared 10 mM solution of glutathione (50 μL) was mixed thoroughly with 1.9 mL 0.1 M TRIS-citrate buffer (pH 7.5), which was then added to 50 μL of freshly prepared KAUS-12, KAUS-15 or ECA (10 mM in DMSO) to initiate the reaction. After a specified time (0 min, 60 min and 180 min), 0.4 mL of the reaction mixture was transferred to a vessel containing 40 μL phosphoric acid (10% in water) and mixed thoroughly. The GSH conjugate with KAUS-12, KAUS-15 or ECA was then detected using LC-MS. A similar reaction procedure, but only studied at one time point of 3 hour, was performed for the free amino acids (L-Cys, L-Val, L-His and L-Lys), and the conjugate formation followed using UPLC-MS.

The LC-MS system was composed of an Agilent 1200 HPLC system, a solvent delivery module, a quaternary pump, an auto-

sampler, and a column compartment (Agilent Technology, Germany). The column effluent was connected to an Agilent 6320 Ion Trap-ESI-MS. The column heater was set to 25 ± 2 °C. The control of the HPLC system and data processing were performed using ChemStation (Rev. B.01.03 SR2-204) and 6300 Series Trap Control version 6.2 Build no. 62.24 (Bruker Daltonik GmbH). The analytes were separated using an Agilent Zorbax Extend-C18 column (80 Å, 150 mm length × 4.6 mm, i.d., 5 μm) and an Agilent-Zorbax Extend-C18 pre-column (Agilent Technologies, Palo Alto, CA, USA). General MS adjustments were set as follows: capillary voltage, 4000 V; nebulizer, 35 psi; drying gas, 12 L min^{-1}; desolvation temperature, 350 °C; ion charge control (ICC) smart target, 150 000; and max accumulation time, 150 ms. Auto-MS positive mode was applied. Mobile system: isocratic elution using 55% acetonitrile and 45% water containing 0.1% formic acid (w/v).

The UPLC-MS analysis was performed using an Acquity H-Class UPLC connected to a PDA detector and an Acquity TQD detector. The column used was an Acquity UPLC BEH C18 1.7 μm, 2.1 × 50 mm, with a Vanguard pre-column attached. Solvent A consisted of 90 : 10 water : acetonitrile with 0.1% formic acid, while solvent B consisted of 90 : 10 acetonitrile : water with 0.1% formic acid. A gradient run was performed such that solvent B was increased from 0% B to 100% B from time 0–7 min, followed by washing with 100% B for 5 min and then a return and re-equilibration at 100% A in the final 3 min (total run time = 15 min). 10 μL of sample was injected per run. The eluent of the column was connected to a PDA UV detector which scanned from 250–350 nm and a 2D channel of 280 nm was used for quantification of compound and adduct. The eluent was then introduced into the TQD detector to confirm the masses of adducts formed. The TQD detector was set to positive ionization mode with a capillary voltage of 3.20 kV, cone voltage of 20 V, extractor voltage of 3 V, and RF lens voltage of 0.1 V. The source temperature was set at 150 °C, while the desolvation temperature was set at 350 °C and the desolvation and cone gas flows were set at 650 and 50 L h^{-1}, respectively. Scans were made from 100–700 m/z with a scan duration of 0.5 seconds to obtain mass spectra at different time points.

Reactivity of KAUS-15 toward βCys93 of Hb. The accessible sulfhydryl groups in Hb, and their reactivity with the test compounds, were quantified by observing the results of the disulfide exchange reaction of the thiols of βCys93 and DTNB at 412 nm (ε = 14 150 M^{-1} cm^{-1}). An aqueous solution of Hb (50 μM tetramer) was mixed with KAUS-15 or ECA (2 mM) in PBS or no compound, and the mixture incubated for four hours at 25 °C. The mixture was centrifuged with washing (PBS) to separate Hb from excess reagents using centrifugal filters (cut off: 10 kDa, Millipore) at 5000 rpm for 30 min at 4 °C. The washed hemoglobin was stored at 4 °C. 10 μl of each Hb solution was diluted to 500 μl in 0.1 M potassium phosphate buffer at pH 8.0 and incubated at 25 °C for 1 h (non-DTNB control). To another set, 10 μl of 10 mM DTNB was added and incubated under similar conditions. Both sets of tubes were centrifuged using centrifugal filters to collect the yellow filtrate (2-nitrobenzoate), which was quantified by measuring absorbance at 412 nm.

Cytotoxicity assessment against C-166 mouse fibroblast cell line. The cytotoxicities of the test compounds, including KAUS-12, KAUS-15 and ECA, were tested against C-166 cells by sulforhodamine B (SRB) colorimetric assay as previously described.[55] Exponentially growing cells were collected using 0.25% Trypsin-EDTA and plated in 96-well plates at 1000–2000 cells per well. Cells were exposed to test compounds for 72 h and subsequently fixed with TCA (10%) for 1 h at 4 °C. After several washings, the cells were exposed to 0.4% SRB solution for 10 min in a dark place and subsequently washed with 1% glacial acetic acid. After drying overnight, Tris-HCl was used to dissolve the SRB-stained cells and the color intensity was measured at 540 nm. All cytotoxicity measurements were repeated thrice (n = 3). The dose response curve of the compounds was analyzed using the E_{max} model.

$$\%\,\text{Cell viability} = (100 - R) \times \left(1 - \frac{[D]^m}{K_d{}^m + [D]^m}\right) + R$$

where R is the residual unaffected fraction (the resistance fraction), [D] is the drug concentration used, K_d is the drug concentration that produces a 50% reduction of the maximum inhibition rate and m is a Hill-type coefficient. The IC_{50} was defined as the drug concentration required to reduce the fluorescence to 50% of that of the control (*i.e.*, $K_d = IC_{50}$ when R = 0 and $E_{max} = 100 - R$).[52]

Acknowledgements

The authors thank Dr Ahmed Al-Abd, Prof. Dr Alaa Khedr and Dr Ali Alhalawany, Faculty of Pharmacy, King Abdulaziz University, for generous support in performing the cell viability (A. Al-Abd) and GSH reactivity (A. Khedr for LC-MS and A. Alhalawany for HPLC) tests, and Dr Akul Mehta at the Virginia Commonwealth University for UPLC-MS analysis of free amino acid conjugates of the test compounds. The authors also thank the Science and Technology Unit, King Abdulaziz University for technical support. This work was supported by the NSTIP strategic technologies program in the Kingdom of Saudi Arabia, Project No. 10-BIO1253-03, NIH/NIMHD grant MD009124 (MKS, OA); NIH/NHLBI grant K01HL103186 (OA). Structural biology resources were provided in part by NIH grant CA16059 to the VCU Massey Cancer Center.

References

1 I. Akinsheye and E. S. Klings, Sickle cell anemia and vascular dysfunction: the nitric oxide connection, *J. Cell. Physiol.*, 2010, **224**, 620.
2 L. De Franceschi, Pathophisiology of sickle cell disease and new drugs for the treatment, *Mediterr. J. Hematol. Infect. Dis.*, 2009, **1**, e2009024.

3 A. Turhan, L. A. Weiss, N. Mohandas, B. S. Coller and P. S. Frenette, Primary role for adherent leukocytes in sickle cell vascular occlusion: a new paradigm, *Proc. Natl. Acad. Sci. U. S. A.*, 2002, **99**, 3047.
4 M. F. Perutz, A. J. Wilkinson, M. Paoli and G. G. Dodson, The stereochemical mechanism of the cooperative effects in hemoglobin revisited, *Annu. Rev. Biophys. Biomol. Struct.*, 1998, **27**, 1.
5 M. F. Perutz, Mechanisms of cooperativity and allosteric regulation in proteins, *Q. Rev. Biophys.*, 1989, **22**, 139.
6 M. F. Perutz, Nature of haem-haem interaction, *Nature*, 1972, **237**, 495.
7 M. K. Safo, M. H. Ahmed, M. S. Ghatge and T. Boyiri, Hemoglobin-ligand binding: Understanding Hb function and allostery on atomic level, *Biochim. Biophys. Acta*, 2011, **1814**, 797.
8 M. K. Safo and S. Bruno, Allosteric Effectors of Hemoglobin: Past, Present and Future, in *Chemistry and Biochemistry of Oxygen Therapeutics: From Transfusion to Artificial Blood*, ed. A. Mozzarelli and S. Bettati, John Wiley & Sons, Ltd, 2011, pp. 285–300.
9 V. Richard, G. G. Dodson and Y. Mauguen, Human deoxyhaemoglobin-2,3-diphosphoglycerate complex low-salt structure at 2.5 A resolution, *J. Mol. Biol.*, 1993, **233**, 270.
10 M. K. Safo and G. J. Kato, Therapeutic strategies to alter the oxygen affinity of sickle hemoglobin, *Hematol. Oncol. Clin. North Am.*, 2014, **28**, 217.
11 O. Abdulmalik, M. S. Ghatge, F. N. Musayev, A. Parikh, Q. Chen, J. Yang, I. N. Nnamani, R. Danso-Danquah, D. N. Eseonu, K. Asakura, D. J. Abraham, J. Venitz and M. K. Safo, Crystallographic analysis of human hemoglobin elucidates the structural basis of the potent and dual antisickling activity of pyridyl derivatives of vanillin, *Acta Crystallogr., Sect. D: Biol. Crystallogr.*, 2011, **67**, 920.
12 M. K. Safo, C. M. Moure, J. C. Burnett, G. S. Joshi and D. J. Abraham, High-resolution crystal structure of deoxy hemoglobin complexed with a potent allosteric effector, *Protein Sci.*, 2001, **10**, 951.
13 I. Lalezari, S. Rahbar, P. Lalezari, G. Fermi and M. F. Perutz, LR16, a compound with potent effects on the oxygen affinity of hemoglobin, on blood cholesterol, and on low density lipoprotein, *Proc. Natl. Acad. Sci. U. S. A.*, 1988, **85**, 6117.
14 F. C. Wireko, G. E. Kellogg and D. J. Abraham, Allosteric modifiers of hemoglobin. 2. Crystallographically determined binding sites and hydrophobic binding/interaction analysis of novel hemoglobin oxygen effectors, *J. Med. Chem.*, 1991, **34**, 758.
15 W. N. Poillon, B. C. Kim, E. V. Welty and J. A. Walder, The effect of 2,3-diphosphoglycerate on the solubility of deoxyhemoglobin S, *Arch. Biochem. Biophys.*, 1986, **249**, 301.
16 W. N. Poillon and B. C. Kim, 2,3-Diphosphoglycerate and intracellular pH as interdependent determinants of the physiologic solubility of deoxyhemoglobin S, *Blood*, 1990, **76**, 1028.
17 O. Abdulmalik, M. K. Safo, Q. Chen, J. Yang, C. Brugnara, K. Ohene-Frempong, D. J. Abraham and T. Asakura, 5-Hydroxymethyl-2-Furfural Modifies Intracellular Sickle Haemoglobin and Inhibits Sickling of Red Blood Cells, *Br. J. Haematol.*, 2005, **128**, 552.
18 M. K. Safo, O. Abdulmalik, R. Danso-Danquah, J. C. Burnett, S. Nokuri, G. S. Joshi, F. N. Musayev, T. Asakura and D. J. Abraham, Structural basis for the potent antisickling effect of a novel class of five-membered heterocyclic aldehydic compounds, *J. Med. Chem.*, 2004, **47**, 466.
19 D. J. Abraham, A. S. Mehanna, F. C. Wireko, J. Whitney, R. P. Thomas and E. P. Orringer, Vanillin, a potential agent for the treatment of sickle cell anemia, *Blood*, 1991, **77**, 1334.
20 R. H. Zaugg, J. A. Walder and I. M. Klotz, Schiff base adducts of hemoglobin. Modifications that inhibit erythrocyte sickling, *J. Biol. Chem.*, 1977, **252**, 8542.
21 M. F. Perutz, G. Fermi, C. Poyart, J. Pagnier and J. Kister, A novel allosteric mechanism in haemoglobin. Structure of bovine deoxyhaemoglobin, absence of specific chloride-binding sites and origin of the chloride-linked Bohr effect in bovine and human haemoglobin, *J. Mol. Biol.*, 1993, **233**, 536.
22 G. Fermi, Three-dimensional fourier synthesis of human deoxyhaemoglobin at 2.5 Å resolution: refinement of the atomic model, *J. Mol. Biol.*, 1975, **97**, 237.
23 S. Park, B. L. Hayes, F. Marankan, D. C. Mulhearn, L. Wanna, A. D. Mesecar, B. D. Santarsiero, M. E. Johnson and D. L. Venton, Regioselective covalent modification of hemoglobin in search of antisickling agents, *J. Med. Chem.*, 2003, **46**, 936.
24 A. Nakagawa, F. E. Lui, D. Wassaf, R. Yefidoff-Freedman, D. Casalena, M. A. Palmer, J. Meadows, A. Mozzarelli, L. Ronda, O. Abdulmalik, K. D. Bloch, M. K. Safo and W. M. Zapol, Identification of a small molecule that increases hemoglobin oxygen affinity and reduces SS erythrocyte sickling, *ACS Chem. Biol.*, 2014, **9**, 2318.
25 H. Hou, N. Khan, O. Y. Grinberg, H. Yu, S. A. Grinberg, S. Lu, E. Demidenko, R. P. Steffen and H. M. Swartz, The effects of Efaproxyn (efaproxiral) on subcutaneous RIF-1 tumor oxygenation and enhancement of radiotherapy-mediated inhibition of tumor growth in mice, *Radiat. Res.*, 2007, **168**, 218.
26 S. R. Khandelwal, R. S. Randad, P. S. Lin, H. Meng, R. N. Pittman, H. A. Kontos, S. C. Choi, D. J. Abraham and R. Schmidt-Ullrich, Enhanced oxygenation in vivo by allosteric inhibitors of hemoglobin saturation, *Am. J. Physiol.*, 1993, **265**, H1450.
27 M. P. Kunert, J. F. Liard and D. J. Abraham, RSR-13, an allosteric effector of hemoglobin, increases systemic and iliac vascular resistance in rats, *Am. J. Physiol.*, 1996, **271**, H602.
28 J. H. Suh, B. Stea, A. Nabid, J. J. Kresl, A. Fortin, J. P. Mercier, N. Senzer, E. L. Chang, A. P. Boyd, P. J. Cagnoni and E. Shaw, Phase III study of efaproxiral as

an adjunct to whole-brain radiation therapy for brain metastases, *J. Clin. Oncol.*, 2006, **24**, 106.

29 D. J. Abraham, M. K. Safo, T. Boyiri, R. E. Danso-Danquah, J. Kister and C. Poyart, How allosteric effectors can bind to the same protein residue and produce opposite shifts in the allosteric equilibrium, *Biochemistry*, 1995, **34**, 15006.

30 T. Boyiri, M. K. Safo, R. E. Danso-Danquah, J. Kister, C. Poyart and D. J. Abraham, Bisaldehyde allosteric effectors as molecular ratchets and probes, *Biochemistry*, 1995, **34**, 15021.

31 I. Lalezari, P. Lalezari, C. Poyart, M. Marden, J. Kister, B. Bohn, G. Fermi and M. F. Perutz, New effectors of human hemoglobin: structure and function, *Biochemistry*, 1990, **29**, 1515.

32 M. K. Safo, T. Boyiri, J. C. Burnett, R. Danso-Danquah, C. M. Moure, G. S. Joshi and D. J. Abraham, X-ray crystallographic analyses of symmetrical allosteric effectors of hemoglobin: compounds designed to link primary and secondary binding sites, *Acta Crystallogr., Sect. D: Biol. Crystallogr.*, 2002, **58**, 634.

33 D. J. Abraham, F. C. Wireko, R. S. Randad, C. Poyart, J. Kister, B. Bohn, J. F. Liard and M. P. Kunert, Allosteric modifiers of hemoglobin: 2-[4-[[(3,5-disubstituted anilino)-carbonyl]methyl]phenoxy]-2-methylpropionic acid derivatives that lower the oxygen affinity of hemoglobin in red cell suspensions, in whole blood, and in vivo in rats, *Biochemistry*, 1992, **31**, 9141.

34 T. Yokoyama, S. Neya, A. Tsuneshige, T. Yonetani, S. Y. Park and J. R. Tame, R-state haemoglobin with low oxygen affinity: crystal structures of deoxy human and carbonmonoxy horse haemoglobin bound to the effector molecule L35, *J. Mol. Biol.*, 2006, **356**, 790.

35 Q. Chen, I. Lalezari, R. L. Nagel and R. E. Hirsch, Liganded hemoglobin structural perturbations by the allosteric effector L35, *Biophys. J.*, 2005, **88**, 2057.

36 N. Shibayama, S. Miura, J. R. Tame, T. Yonetani and S. Y. Park, Crystal structure of horse carbonmonoxyhemoglobin-bezafibrate complex at 1.55 Å resolution, A novel allosteric binding site in R-state hemoglobin, *J. Biol. Chem.*, 2002, **277**, 38791.

37 P. E. Kennedy, F. L. Williams and D. J. Abraham, Design, synthesis, and testing of potential antisickling agents. 3. Ethacrynic acid, *J. Med. Chem.*, 1984, **27**, 103.

38 M. F. Perutz, G. Fermi, D. J. Abraham, C. Poyart and E. Bursaux, Hemoglobin as a receptor of drugs and peptides: x-ray studies of the stereochemistry of binding, *J. Am. Chem. Soc.*, 1986, **108**, 1064.

39 R. S. Garcia, C. Pietra, C. Giuliano and Z. Li, Asymmetric ureas and medical uses thereof, *Patent EP*, 2678017A2, 2014.

40 A. Vass, J. Dudas, L. Borbely, F. Haasz and P. Jekkel, A new process for the preparation of phenolic hydroxy-substituted compounds, *Patent WO*, 2006061666A2, 2006.

41 S. Hack, B. Worlein, G. Hofner, J. Pabel and K. T. Wanner, Development of imidazole alkanoic acids as mGAT3 selective GABA uptake inhibitors, *Eur. J. Med. Chem.*, 2011, **46**, 1483.

42 N. C. Kaarsholm, O. H. Birk, P. Madsen, S. Oestergaard, P. Jakobsen and T. T. Moeller, Pharmaceutical preparations comprising insulin, zinc ions and a zinc-binding ligand, *Patent WO*, 2006082245A1, 2006.

43 H. R. Lawrence, S. Ozcan and S. M. Sebti, Proteasome chymotrypsin-like inhibition using pi-1833 analogs, WO 2012129564A2, 2012.

44 K. L. Kirk, Facile synthesis of 2-substituted imidazoles, *J. Org. Chem.*, 1978, **43**, 4381.

45 J. C. Chapuis, O. Khdour, X. Cai, J. Lu and S. M. Hecht, Synthesis and characterization of Deltalac-acetogenins that potently inhibit mitochondrial complex I, *Bioorg. Med. Chem.*, 2009, **17**, 2204.

46 M. K. Safo and D. J. Abraham, X-ray crystallography of hemoglobins, *Methods Mol. Med.*, 2003, **82**, 1.

47 E. Chiancone, D. L. Currell, P. Vecchini, E. Antonini and J. Wyman, Kinetics of the reaction of the "masked" and "free" sulfhydryl groups of human hemoglobin with p-mercuribenzoate, *J. Biol. Chem.*, 1970, **245**, 4105.

48 M. A. Padmos, G. T. Roberts, K. Sackey, A. Kulozik, S. Bail, J. S. Morris, B. E. Serjeant and G. R. Serjeant, Two different forms of homozygous sickle cell disease occur in Saudi Arabia, *Br. J. Haematol.*, 1991, **79**, 93.

49 M. A. El-Hazmi, Heterogeneity and variation of clinical and haematological expression of haemoglobin S in Saudi Arabs, *Acta Haematol.*, 1992, **88**, 67.

50 M. E. Pembrey, W. G. Wood, D. J. Weatherall and R. P. Perrine, Fetal haemoglobin production and the sickle gene in the oases of Eastern Saudi Arabia, *Br. J. Haematol.*, 1978, **40**, 415.

51 E. Boyland and L. F. Chasseaud, The role of glutathione and glutathione S-transferases in mercapturic acid biosynthesis, *Adv. Enzymol. Relat. Areas Mol. Biol.*, 1969, **32**, 173.

52 M. D. Winn, C. C. Ballard, K. D. Cowtan, E. J. Dodson, P. Emsley, P. R. Evans, R. M. Keegan, E. B. Krissinel, A. G. Leslie, A. McCoy, S. J. McNicholas, G. N. Murshudov, N. S. Pannu, E. A. Potterton, H. R. Powell, R. J. Read, A. Vagin and K. S. Wilson, Overview of the CCP4 suite and current developments, *Acta Crystallogr., Sect. D: Biol. Crystallogr.*, 2011, **67**, 235.

53 A. T. Brunger, P. D. Adams, G. M. Clore, W. L. DeLano, P. Gros, R. W. Grosse-Kunstleve, J. S. Jiang, J. Kuszewski, M. Nilges, N. S. Pannu, R. J. Read, L. M. Rice, T. Simonson and G. L. Warren, Crystallography & NMR system: A new software suite for macromolecular structure determination, *Acta Crystallogr., Sect. D: Biol. Crystallogr.*, 1998, **54**, 905.

54 P. Emsley and K. Cowtan, Coot: model-building tools for molecular graphics, *Acta Crystallogr., Sect. D: Biol. Crystallogr.*, 2004, **60**, 2126.

55 P. Skehan, R. Storeng, D. Scudiero, A. Monks, J. McMahon, D. Vistica, J. T. Warren, H. Bokesch, S. Kenney and M. R. Boyd, New colorimetric cytotoxicity assay for anticancer-drug screening, *J. Natl. Cancer Inst.*, 1990, **82**, 1107.

